Author Manuscript

Author Manuscript

Author Manuscript

Author Manuscript

HHS Public Access

Author manuscript

Immunity. Author manuscript; available in PMC 2022 February 09.

Published in final edited form as:

Immunity. 2021 February 09; 54(2): 308–323.e6. doi:10.1016/j.immuni.2020.12.010.

The TGF-β superfamily cytokine Activin-A is induced during autoimmune neuroinflammation and drives pathogenic Th17 cell differentiation

Bing Wu[1,2], **Song Zhang**[1,2], **Zengli Guo**[1,2], **Yanmin Bi**[3], **Mingxia Zhou**[1,2], **Ping Li**[1,2], **Maryamsadat Seyedsadr**[4], **Xiaojiang Xu**[5], **Jian-liang Li**[5], **Silva Markovic-Plese**[4], **Yisong Y Wan**[1,2,6,*]

[1]Lineberger Comprehensive Cancer Center, School of Medicine, University of North Carolina at Chapel Hill, North Carolina 27599, USA;

[2]Department of Microbiology and Immunology, School of Medicine, University of North Carolina at Chapel Hill, North Carolina 27599, USA;

[3]Gene Therapy Center, University of North Carolina at Chapel Hill, Chapel Hill, NC, 27599, USA;

[4]Department of Neurology, Thomas Jefferson University, Philadelphia, PA, 19107, USA;

[5]Integrative Bioinformatics, National Institute of Environmental Health Sciences, Research Triangle Park, North Carolina 27709, USA;

[6]Lead contact.

Summary

Th17 cells are known to exert both pathogenic and non-pathogenic functions. While the cytokine TGF-β1 is instrumental to Th17 cell differentiation, it is dispensible for the generation of pathogenic-Th17 cells. Here, we examined the T cell-intrinsic role of Activin-A, a TGF-β superfamily member closely related to TGF-β1, in pathogenic-Th17 cell differentiation. Activin-A expression was increased in patients with relapsing-remitting multiple sclerosis, and in mice with experimental autoimmune encephalomyelitis. Stimulation with interleukin-6 and Activin-A induced a molecular program that mirrored that of pathogenic-Th17 cells, which was inhibited by blocking Activin-A signaling. Genetic disruption of Activin-A and its receptor ALK4 in T cells impaired pathogenic-Th17 cell differentiation *in vitro* and *in vivo*. Mechanistically, ERK

*Correspondence: wany@email.unc.edu.

Author contribution:

B.W. contributed to the design, the cellular, molecular, biochemical and animal experiments, and the writing of the manuscript; S.Z. contributed to the plasmid construction and *in vitro* analysis; M.Z. contributed to the immune-blotting and qRT-PCR experiments; P.L. contributed to RNA-seq sample preparations; Z.G., Y.B., X.X. and J.L. contributed to bioinformatic analysis; S.M.P. and M.S. contributed to human samples study; Y.Y.W. conceived the project, designed experiments, and wrote the manuscript.

Publisher's Disclaimer: This is a PDF file of an unedited manuscript that has been accepted for publication. As a service to our customers we are providing this early version of the manuscript. The manuscript will undergo copyediting, typesetting, and review of the resulting proof before it is published in its final form. Please note that during the production process errors may be discovered which could affect the content, and all legal disclaimers that apply to the journal pertain.

Declaration of interests

The authors declare no competing financial interests.

SUPPLEMENTAL INFORMATION is linked to the online version of the paper.

Author Manuscript Author Manuscript Author Manuscript Author Manuscript

phosphorylation, which was essential for pathogenic-Th17 cell differentiation, was suppressed by TGF-β1-ALK5 but not Activin-A-ALK4 signaling. Thus, Activin-A drives pathogenic-Th17 cell differentiation, implicating the Activin-A-ALK4-ERK axis as a therapeutic target for Th17 cell-related diseases.

Graphical Abstract

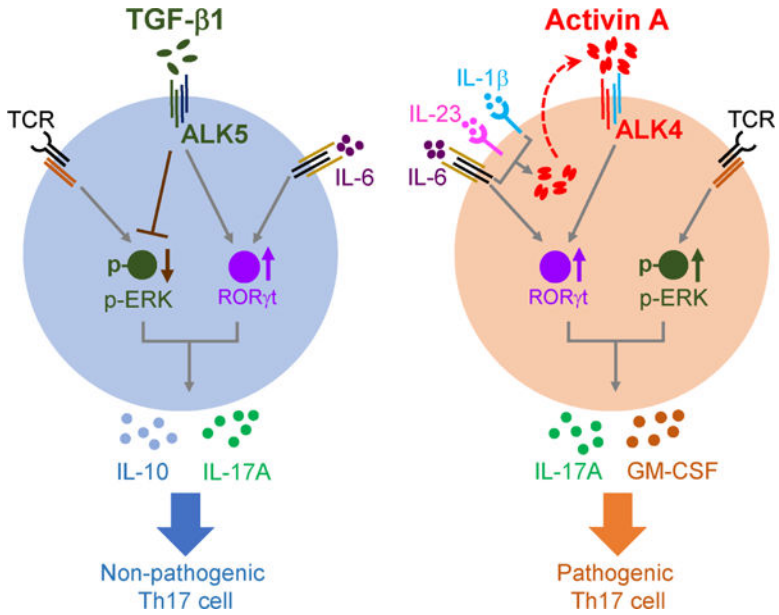

In Brief

Identifying factors controlling pathogenic-Th17 cells is critical due to their roles in disease and autoimmunity. Wu et al. demonstrate T cell-intrinsic Activin-A signaling, but not closely related TGF-β1, drives pathogenic-Th17 cell differentiation and function during autoimmunity. This points to Activin-A as a potential therapeutic target in pathogenic Th-17-mediated diseases.

Keywords

autoimmune disease; multiple sclerosis; EAE; pathogenic Th17 cells; Activin-A; ALK4; TGF-β1; ALK5; ERK1/2

Introduction

IL-17A-producing helper T (Th17) cells were initially identified as pathogenic cells for tissue inflammation and autoimmune disease (Dong, 2006; Korn et al., 2009; Weaver et al., 2006). It is now clear that Th17 cells also have non-pathogenic, immune-regulatory function (Esplugues et al., 2011; McGeachy et al., 2007; Omenetti et al., 2019). Owing to the broad functions of Th17 cells in immune regulation and disease, it is of great importance to understand how the generation and function of Th17 cells are controlled, particularly the dichotomy between the pathogenic-Th17 vs. non-pathogenic-Th17 cells (Gaublomme et al.,

Author Manuscript Author Manuscript Author Manuscript Author Manuscript

2015; Lee et al., 2020; Lee et al., 2012; Stockinger and Omenetti, 2017; Wang et al., 2015; Wang et al., 2020).

Pathogenic- and non-pathogenic-Th17 cells can be differentiated *in vitro* in the context of different cytokines (Stockinger and Omenetti, 2017). IL-6+IL-23+IL-1β drive pathogenic-Th17 (Ghoreschi et al., 2010; Lee et al., 2012), whereas TGF-β1+IL-6 drive non-pathogenic-Th17 cell differentiation (Bettelli et al., 2006; Mangan et al., 2006; McGeachy et al., 2007; Veldhoen et al., 2006). While both pathogenic- and non-pathogenic-Th17 cells express Th17 cell signature molecules including IL-17A and RORγt, they adopt distinct genetic programs that contribute to either immune pathology or immune homeostasis (Ghoreschi et al., 2011; Stockinger and Omenetti, 2017). Pathogenic-Th17 cells express high amounts of pro-inflammatory molecules including GM-CSF and IL-23R and low amounts of immune regulatory molecules including IL-10 and CD5L. In contrast, non-pathogenic-Th17 cells express low amounts of GM-CSF, IL-23R and high amounts of IL-10 and CD5L to promote tissue homeostasis (Gaublomme et al., 2015; Lee et al., 2012; McGeachy et al., 2007; Omenetti et al., 2019; Wang et al., 2015).

The TGF-β superfamily is composed of more than 30 structurally related molecules including TGF-βs, bone morphogenetic proteins (BMPs), Activins, and growth and differentiation factors (GDFs) (Chen and Ten Dijke, 2016; Weiss and Attisano, 2013). Although TGF-β related signaling is instrumental to the differentiation of Th17 cells *in vitro* and *in vivo* (Bettelli et al., 2006; Gutcher et al., 2011; Li et al., 2007; Mangan et al., 2006; McGeachy et al., 2007), its role in pathogenic-Th17 cells remains controversial. TGF-β1 and its specific receptor ALK5 are dispensable for the generation of pathogenic-Th17 cells (Ghoreschi et al., 2010). Yet, TGF-β related cytokines and the shared Smad2, Smad4 and SKI pathways are important for the pathogenicity of Th17 cells (Martinez et al., 2010; Wang et al., 2020; Zhang et al., 2017). How different TGF-β superfamily members regulate T cell function remains unclear.

Activin-A encoded by *Inhba* gene is a pleiotropic cytokine closely related to TGF-β1 that has diverse, sometimes opposing, cellular functions in a context dependent manner (Chen and Ten Dijke, 2016; Morianos et al., 2019; Weiss and Attisano, 2013). Activin-A binds to its specific type-I receptor ALK4, whereas TGF-β1 binds to ALK5, to initiate signaling, gene expression, and the function of target cells through similar yet distinct pathways (David and Massague, 2018; Derynck and Budi, 2019; Heldin and Moustakas, 2016). Both Activin-A and TGF-β1 induce the phosphorylation of Smad2 and Smad3 and the degradation of SKI protein (Derynck and Budi, 2019; Zhang et al., 2017). Yet, Activin-A and TGF-β1 can activate different MAPK signaling in the same cell type (Bauer et al., 2015; Moustakas and Heldin, 2005; Tsuchida et al., 2009). Activin-A not only promotes the generation and function of immune suppressive regulatory T (Treg) cells by synergizing with TGF-β1 (Huber et al., 2009), but also promotes pro-inflammatory Th2-, Th9- and Tfh-related responses (Jones et al., 2012; Locci et al., 2016; Ogawa et al., 2006). Of interest, increased Activin-A is associated with Th17 cell mediated inflammatory diseases including inflammatory bowel disease, rheumatoid arthritis, and asthma (Korn et al., 2009; Phillips et al., 2009; Sideras et al., 2013; Werner and Alzheimer, 2006). Such a correlation and the fact

Author Manuscript Author Manuscript Author Manuscript Author Manuscript

that Activin-A, like TGF-β1, can induce Th17 differentiation *in vitro* (Zhang et al., 2017) suggest that Activin-A may be involved in Th17 cell-mediated pathogenesis.

In this study, we found that Activin-A was increased in the sera of untreated relapsing-remitting multiple sclerosis (RRMS) patients and of mice with experimental autoimmune encephalitis (EAE), a mouse model for human MS. The expression of Activin-A, but not TGF-β1, was increased in central nervous system (CNS) infiltrating T cells. Activin-A expression was induced in T cells by inflammatory cytokines IL-6, IL-23, and IL-1β, and was required for pathogenic- but not non-pathogenic-Th17 cell differentiation. T cell-derived Activin-A was critical for the induction of pathogenic-Th17 cell-mediated EAE. In addition, T cells activated in the presence of Activin-A+IL-6 adopted a genetic program nearly identical to pathogenic-Th17 cells and potently elicited severe EAE. Moreover, increased ALK4 expression and decreased ALK5 expression in activated T cells during inflammation sustained the ability of Activin-A, but not TGF-β1, to promote pathogenic-Th17 cell differentiation and EAE. Conversely, TGF-β1 but not Activin-A suppressed ERK phosphorylation that was essential for the differentiation of pathogenic-Th17 cells. This study sheds lights on distinct roles for Activin-A and TGF-β1 in directing pathogenic- and non-pathogenic-Th17 cell differentiation, respectively, and uncovers therapeutic targets to suppress pathogenic-Th17 cell function and inflammatory diseases.

Results

Neuroinflammation and pathogenic-Th17 cell differentiation increased Activin-A expression in T cells.

Since Activin-A has been implicated in inflammatory diseases, we investigated if Activin-A expression was associated with autoimmune neuroinflammation in patients with relapse remitting multiple sclerosis (RRMS), and in mice with experimental autoimmune encephalitis (EAE). Activin-A protein was elevated in the serum of recently diagnosed untreated RRMS patients in comparison to healthy controls (HCs) (Fig. 1A). Similarly, Activin-A was increased in both serum and the supernatant of spinal cord tissue of mice with EAE (Fig. 1B, 1C). Of note, the mRNA amounts of *Inhba*, but not *Tgfb*(s), progressively increased in the spinal cord-infiltrating $CD4^+$ T cells with the worsening of EAE (Fig. 1D and Supplemental Fig. 1A, 1B), suggesting that inflammatory conditions promoted Activin-A expression in $CD4^+$ T cells. Indeed, various combinations of inflammatory cytokines IL-6, IL-23, and IL-1β induced *Inhba* expression (Fig. 1E) in activated $CD4^+$ T cells *in vitro*. Since IL-6+IL-23+IL-1β polarize pathogenic-Th17 cells (Ghoreschi et al., 2010; Lee et al., 2012), we wondered to what extent Activin-A production was associated with pathogenic-Th17 cell differentiation. We found that T cell-secreted Activin-A was greatly increased during the differentiation of pathogenic-Th17, but not non-pathogenic-Th17 cells (Fig. 1F and Supplemental Fig. 1C). These findings were unexpected because TGF-β1, a cytokine closely related to Activin-A and belonging to the same TGF-β superfamily, is dispensable for pathogenic-Th17 cells (Ghoreschi et al., 2010). To confirm that T cell-secreted Activin-A indeed stimulated downstream signaling, we assessed SKI protein reduction, a sensitive readout for Activin-A signaling (Zhang et al., 2017). During pathogenic-Th17 cell differentiation, SKI protein level was reduced (Fig. 1G), which was

Author Manuscript Author Manuscript Author Manuscript Author Manuscript

prevented by antibody-mediated neutralization of Activin-A (Fig. 1H) but not TGF-β1 (Fig. 1I–J). This observation indicated Activin-A induced pathogenic-Th17 cell differentiation, while TGF-β1 was dispensable (Ghoreschi et al., 2010).

Activin-A was required for pathogenic-Th17 cell differentiation *in vitro*.

To address if Activin-A was important for pathogenic-Th17 cell differentiation *in vitro*, we neutralized Activin-A when $CD4^+$ T cells were activated in the presence of IL-6+IL-23+IL-1β. Activin-A neutralization led to reduced Th17 cell differentiation (Fig. 2A, 2B), decreased expression of pathogenic-Th17 cell genes *Il23r* and *Csf2*, and production of GM-CSF protein, but increased expression of non-pathogenic-Th17 cell genes *Il10* and *Cd5l* and production of IL-10 protein (Fig. 2B and Supplemental Fig. 2A, 2B). Such an effect was specific for pathogenic-Th17 cells as Activin-A neutralization did not affect TGF-β1+IL-6 induced non-pathogenic Th17 cell differentiation (Supplemental Fig. 2C–F). Consistently, using genome-wide RNA-seq analysis, we found that Activin-A neutralization inhibited IL-6+IL-23+IL-1β-promoted pathogenic-Th17 cell program (Supplemental Fig. 2G–H). In addition, we blocked Activin-A's binding to its receptor by using Follistatin, a natural Activin-A antagonist that can improve various inflammatory diseases (de Kretser et al., 2012; Harrison et al., 2005; Hedger and de Kretser, 2013). Addition of recombinant Follistatin (rFst) hampered pathogenic-Th17 cell differentiation (Fig. 2C, 2D and Supplemental Fig. 2I–J) but not non-pathogenic Th17 cell differentiation (Supplemental Fig. 2K). Similarly, retrovirus-mediated ectopic expression of Follistatin in activated T cells (Supplemental Fig. 2L) decreased the differentiation of pathogenic- but not non-pathogenic-Th17 cells (Supplemental Fig. 2M–Q).

We next investigated if T cell-produced Activin-A was important for pathogenic-Th17 cell differentiation *in vitro*. To this end, we performed shRNA-mediated RNAi of *Inhba* in $CD4^+$ T cells under pathogenic-Th17 cell polarizing condition, using lentivirus-mediated shRNA expression (Supplemental Fig. 2R). Reduced expression of Activin-A in T cells led to reduced pathogenic-Th17 cell differentiation (Fig. 2E), decreased gene expression of *Il23r*, *Csf2* and protein production of GM-CSF, but increased gene expression of *Il10*, *Cd5l* and protein production of IL-10 (Fig. 2F and Supplemental Fig. 2S–T). We also performed CRISPR-Cas9-sgRNA mediated genomic editing to disrupt *Inhba* gene expression (Supplemental Fig. 2U) by transducing lentivirus-encoded Activin-A sgRNA into $CD4^+$ T cells that express CRISPR-Cas9 (Platt et al., 2014). Consistent with the results of shRNA-mediated RNAi of *Inhba*, disruption of Activin-A expression in T cells under pathogenic-Th17 cell polarizing condition led to reduced differentiation of pathogenic-Th17 cells (Fig. 2G, 2H, and Supplemental Fig. 2V–W). These results suggested that Activin-A produced by activated T cells in the inflammatory milieu was required for the pathogenic-Th17 cell differentiation.

Autocrine Activin-A was important for pathogenic-Th17 cell-promoted EAE.

We next investigated how T cell-produced Activin-A contributed to pathogenic-Th17 cell differentiation during EAE. To this end, we employed T cell adoptive transfer to elicit EAE (Fig. 3A). We crossed *CD4cre*-dependent-*Cas9*-expressing mice with MOG-peptide-specific 2D2 TCR transgenic mice to obtain *CD4cre;Cas9;2D2* mice. *CD4cre;Cas9;2D2* T cells were

Author Manuscript Author Manuscript Author Manuscript Author Manuscript

differentiated into pathogenic-Th17 cells and transduced with lentiviruses encoding sgRNA and a tracing marker Thy1.1. Transduced T cells were purified and transferred into irradiated wild-type mice. The mice that received Activin-A sgRNA-transduced T cells showed lower incidence, delayed onset, and milder severity of EAE in comparison to mice that received T cells transduced with control sgRNA (Fig. 3B, 3C). Consistent with these results, Activin-A sgRNA-transduced cells expressed much less IL-17A, but not IFN-γ, in the spinal cords of mice with EAE in comparison to control sgRNA-transduced cells (Fig. 3D). To elucidate if Activin-A was required for pathogenic-Th17 cell differentiation during EAE in a cell-intrinsic manner, we transferred both control sgRNA-transduced ($CD45.1^+$) and Activin-A sgRNA-transduced ($CD45.1^+CD45.2^+$) cells into irradiated recipient mice ($CD45.2^+$), followed by EAE induction with $MOG_{35–55}$+CFA (Fig. 3E). Activin-A sgRNA-transduced cells had decreased Th17 cell differentiation in comparison to co-existing control sgRNA-transduced cells (Fig. 3F). Therefore, T cell-produced Activin-A was important for pathogenic-Th17 cell-promoted EAE and functions in an autocrine manner, because Activin-A in the micro-environment was unable to restore the pathogenic-Th17 cell differentiation of Activin-A-deficient T cells during EAE.

Activin-A induced pathogenic-Th17 cells that promote neuroinflammation.

The findings that Activin-A was required for pathogenic-Th17 cell differentiation *in vitro* and *in vivo* made us wonder if Activin-A selectively promoted pathogenic-Th17 cell differentiation. In the presence of IL-6, Activin-A induced Th17 cell differentiation in serum-free medium (Supplemental Fig. 3A), consistent with the genome-wide RNA-seq analysis showing that Activin-A+IL-6 but not IL-6 alone promoted Th17 cell differentiation program (Supplemental Fig. 3B–C). Addition of recombinant Follistatin (Supplemental Fig. 3D) and the ectopic expression of Follistatin in T cells (Supplemental Fig. 3E) inhibited Activin-A+IL-6 differentiated Th17 cells, confirming that it was an Activin-A-mediated effect that is antagonized by Follistatin in T cells. We next performed genome-wide RNA-seq analysis to compare the gene expression profiles of T cells activated in the presence of Activin-A+IL-6 vs. IL-6+IL-23+IL-1β and TGF-β1+IL-6 for 24 and 48 hours. Interestingly, principal-component analysis (PCA) revealed that Activin-A+IL-6-polarized cells were much more similar to IL-6+IL-23+IL-1β-polarized cells than to TGF-β1+IL-6-polarized cells (Fig. 4A). While approximately 3700 differentially expressed genes (DEG) were identified between Activin-A+IL-6-polarized and TGF-β1+IL-6-polarized cells, less than 140 DEGs were identified between Activin-A+IL-6-polarized and IL-6+IL-23+IL-1β-polarized cells (Fig. 4B). Of note, less than 20 genes were differentially expressed by 2-fold or more between Activin-A+IL-6-polarized and IL-6+IL-23+IL-1β-polarized cells, as oppose to more than 930 genes between Activin-A+IL-6-polarized and IL-6+TGF-β1-polarized cells (Supplemental Fig. 3F). Importantly, gene set enrichment analysis (GSEA) using previously defined Th17 cell gene sets (Lee et al., 2012) revealed that Activin-A+IL-6-polarized cells remarkably resembled pathogenic-Th17 cells and were not similar to non-pathogenic-Th17 cells (Fig. 4C). Such an early adoption of pathogenic-Th17 program of Activin-A+IL-6-polarized cells was sustained, as Activin-A+IL-6-polarized cells produced high amounts of *Il17a*, *Rorc*, *Il23r*, *Csf2* mRNA and GM-CSF protein, but low amounts of *Il10*, *Cd5l* mRNA and IL-10 protein 4 days post activation (Fig. 4D, 4E and Supplemental Fig. 3G–I).

Author Manuscript Author Manuscript Author Manuscript Author Manuscript

Using adoptive transfer of 2D2 TCR-transgenic T cells, we compared the encephalitogenic potential of Activin-A+IL-6-polarized vs. TGF-β1+IL-6-polarized Th17 cells (Fig. 4F). We found that, compared to TGF-β1+IL-6-polarized Th17 cells, Activin-A+IL-6-polarized Th17 cells elicited an earlier onset and more severe EAE in recipient mice (Fig 4G, 4H). In addition, transferred Activin-A+IL-6-polarized Th17 cells produced less immunoregulatory cytokine IL-10 than transferred TGF-β1+IL-6-polarized Th17 cells in the spinal cords of mice with EAE (Fig. 4I). These findings suggested that, under inflammatory condition, e.g. in the presence of IL-6, Activin-A could effectively drive the differentiation of highly encephalitogenic Th17 cells.

ALK4 and ALK5 played dichotomous roles in Th17 cell differentiation.

The observation that Activin-A and TGF-β1, albeit closely related, drove the differentiation of Th17 cells with distinct functions prompted us to investigate how ALK4 (type I receptor specific for Activin-A) and ALK5 (type I receptor specific for TGFβ1) were regulated and functioned. The protein expression of ALK4 in the spinal cord infiltrating $CD4^+$ T cells was increased with EAE progression (Fig. 5A). In contrast, the protein expression of ALK5 was reduced in the same cells (Fig. 5A). Consistently, *Alk4* mRNA progressively increased and *Alk5* mRNA moderately decreased in the spinal cord infiltrating $CD4^+$ T cells during EAE development (Supplemental Fig. 4A). In agreement with these *in vivo* findings, ALK4 protein expression was increased in T cells 24 hours after activation, particularly in the presence of inflammatory cytokines, while ALK5 protein expression was decreased (Fig. 5B).

The dichotomous ALK4 and ALK5 expression in activated T cells were functionally important because 24-hour-activated $ALK4^{high}ALK5^{low}$ T cells became much less sensitive to TGF-β1+IL-6-driven Th17 cell differentiation (Supplemental Fig. 4B), but remained sensitive to Activin-A+IL-6-driven Th17 cell differentiation (Supplemental Fig. 4C), as well as to IL-6+IL-23+IL-1β-driven Th17 cell differentiation (Supplemental Fig. 4D) that is independent of TGF-β1 (Ghoreschi et al., 2010). These findings prompted us to posit that ALK4 was important for pathogenic-Th17 cell differentiation. Indeed, CRISPR/Cas9-sgRNA-mediated disruption of ALK4 expression (Supplemental Fig. 4E), which abrogated Activin-A- but not TGF-β1-driven Th17 cell differentiation (Supplemental Fig. 4F, 4G), led to reduced IL-6+IL-23+IL-1β-driven pathogenic-Th17 cell differentiation (Fig. 5C), decreased production of *Il17a*, *Rorc*, *Il23r*, *Csf2* mRNA and GM-CSF protein, and increased production of *Il10* and *Cd5l* mRNA and IL-10 protein (Fig. 5D and Supplemental Fig. 4H–I).

While the dichotomous expression of ALK4 and ALK5 may account for their differential involvement in pathogenic-Th17 cell differentiation, we further investigated if ALK4 and ALK5 signaled differently in driving Th17 cell differentiation. To this end, using retrovirus transduction, we ectopically expressed constitutively-activated (ca) forms of ALK4 (ca-ALK4) bearing T206D mutation and ca-ALK5 bearing T204D mutation in T cells (Supplemental Fig. 4J) to activate downstream signaling such as Smad2 phosphorylation without providing exogenous cytokines (Supplemental Fig. 4K) (Moren et al., 2005; ten Dijke et al., 1994). In the presence of IL-6, ca-ALK4 and ca-ALK5 expression promoted

Author Manuscript Author Manuscript Author Manuscript Author Manuscript

Th17 cell differentiation comparably (Fig. 5E). Interestingly, GSEA of genome-wide RNA-seq datasets revealed that, compared to ca-ALK5 expressing cells, ca-ALK4 expressing cells expressed genes less enriched in IL-10-related programs (Aschenbrenner et al., 2018) (Fig. 5F–H). Compared to ca-ALK4 expressing cells, *Il10* expression was increased in ca-ALK5 expressing cells, although *Il17a* and *Rorc* expression were comparable (Fig. 5I and Supplemental Fig. 4L). Therefore, ALK4 and ALK5 signaling favored pathogenic- and non-pathogenic-Th17 cell differentiation, respectively.

ALK4 directed pathogenic-Th17 cells to promote EAE.

The finding that ALK4 was important for pathogenic-Th17 cell differentiation *in vitro* prompted us to address if ALK4 was important for Th17 cell-induced EAE. *CD4cre;Cas9;2D2* $CD4^+$ T cells were activated under pathogenic-Th17 cell-polarizing condition (IL-6+IL-23+IL-1β) and transduced with lentivirus encoding ALK4 sgRNA to disrupt ALK4 expression. Transduced cells were purified and transferred into irradiated recipients to elicit EAE (Fig. 6A). Compared to control sgRNA-transduced T cells, ALK4 sgRNA-transduced T cells induced EAE with lower incidence, delayed onset, and less severity (Fig. 6B, 6C). Consistent with these clinical results, spinal cord-infiltrating ALK4 sgRNA-transduced T cells produced less IL-17A, comparable IFN-γ, during EAE (Fig. 6D). To further discern if ALK4 was required for pathogenic-Th17 cell differentiation during EAE in a cell-intrinsic manner, we transferred both control sgRNA-transduced T cells ($CD45.1^+$) and ALK4 sgRNA-transduced T cells ($CD45.1^+CD45.2^+$) into irradiated recipient mice ($CD45.2^+$), followed by EAE induction with $MOG_{35–55}$+CFA (Fig. 6E). Compared to the co-exiting control sgRNA-transduced T cells, ALK4 sgRNA-transduced T cells produced less IL-17A in the spinal cords of mice with EAE (Fig. 6F). Therefore, ALK4 was important, in a cell-intrinsic manner, for pathogenic-Th17 cell differentiation to induce EAE.

We found that, in the presence of IL-6, ca-ALK4 and ca-ALK5 expression drove Th17 cell differentiation with distinct molecular program *in vitro* (Fig. 5F–5I). Therefore, we wondered how ca-ALK4 and ca-ALK5 expression may impact EAE development *in vivo*. To this end, we activated and transduced 2D2 T cells with retrovirus encoding ca-ALK4 and ca-ALK5 in the presence of IL-6. Transduced T cells were then purified and transferred into irradiated mice to induce EAE. Compared to ca-ALK5-transduced 2D2 T cells which elicited mild EAE, ca-ALK4-transduced 2D2 T cells elicited EAE with higher incidence, earlier onset, and increased severity (Fig. 6G, 6H). Of interest, although the IL-17A expression was comparable between ca-ALK4- and ca-ALK5-transduced T cells in the spinal cords of mice with EAE (Fig. 6I), ca-ALK5- but not ca-ALK4-transduced T cells expressed high amounts of IL-10 (Fig. 6J). This finding is consistent with what was observed *in vitro* and explains the mild EAE in the recipients of ca-ALK5-transduced T cells (Fig. 5F–5I). Therefore, unlike ALK5, ALK4 critically directed pathogenic-Th17 cell induced EAE.

Author Manuscript Author Manuscript Author Manuscript Author Manuscript

Activin-A permitted and TGF-β1 impeded ERK activation that was critical to endow Th17 cells with pathogenic capacity.

While Activin-A and TGF-β1 are closely related cytokines that can function synergistically to promote Treg cells (Huber et al., 2009), our aforementioned findings revealed an unexpected role for Activin-A signaling to direct pathogenic-Th17 cell differentiation independent of TGF-β1. This was further confirmed by the findings that neutralizing TGF-β1 had no effect on Activn-A+IL-6-driven (Supplemental Fig. 5A) or on IL-6+IL-23+IL-1β-driven (Supplemental Fig. 5B) Th17 cell differentiation, but effectively blocked TGF-β1+IL-6-driven Th17 cell differentiation (Supplemental Fig. 5C). We therefore sought to understand how Activin-A-ALK4 and TGF-β1-ALK5 signaled differently in pathogenic-Th17 cells. By comparative bio-informatic analysis of the RNA-seq datasets between Activin-A+IL-6 vs. TGF-β1+IL-6-stimulated cells, IL-6+IL23+IL-1β vs. TGF-β1+IL-6-stimulated cells, and ca-ALK4 vs. ca-ALK5-expressing cells, we found that ERK signaling pathways were consistently enriched in pathogenic-Th17 cells (Fig. 7A). Because ERK has been implicated in controlling Th17 cell function and inflammation (Brereton et al., 2009; Liu et al., 2013), we interrogated if ERK activation was affected by Activin-A or TGF-β1 during Th17 cell differentiation. ERK phosphorylation was comparable when T cells were stimulated with IL-6+IL23+IL-1β and Activin-A+IL-6 but reduced when T cells were stimulated TGF-β1+IL-6, although STAT3 phosphorylation was similar in all three conditions (Fig. 7B). The inhibitory effect of ERK phosphorylation appeared to be TGF-β1 specific. TGF-β1, but not Activin-A, strongly suppressed ERK phosphorylation during IL-6+IL23+IL-1β-induced pathogenic-Th17 cell differentiation (Fig. 7C). In addition, ectopic expression of ca-ALK5 but not ca-ALK4 inhibited ERK phosphorylation (Fig. 7D).

To further investigate if ERK activation is important for pathogenic-Th17 cell differentiation or function, we inhibited ERK activation and phosphorylation with a pharmacological MEK inhibitor (MEKi). At the dose of 10μM, MEKi inhibited ERK phosphorylation in T cells (Supplemental Fig. 5D) without affecting T cell proliferation or survival (Supplemental Fig. 5E–F). Of interest, Th17 cells differentiated normally with unperturbed expression of *Il17a* and *Rorc* when treated with MEKi (Fig. 7E–7G). Yet, MEKi treatment specifically hampered pathogenic program of Th17 cells, because addition of MEKi during Th17 cell differentiation led to decreased production of *Il23r* and *Csf2* mRNA and GM-CSF protein but increased production of *Il10* and *Cd5l* mRNA and IL-10 protein (Fig. 7H–J and Supplemental Fig. 5G–L).

Collectively, this study demonstrated a previously unappreciated critical role for autocrine Activin-A-ALK4 signal that was distinct from TGF-β1-ALK5 signal in directing pathogenic-Th17 cell differentiation to contribute to autoimmune neuroinflammation (Supplementary Fig. 6).

Discussion

Pathogenic-Th17 cells are critical to drive the development of a myriad of inflammatory and autoimmune diseases including multiple sclerosis (Korn et al., 2009). It is therefore important to understand the mechanism(s) controlling pathogenic-Th17 cell differentiation to aid treatment. We showed that T cell-derived Activin-A was essential to direct

Author Manuscript Author Manuscript Author Manuscript Author Manuscript

pathogenic- but not non-pathogenic-Th17 cell differentiation in an autocrine, ALK4-dependent manner. Thus, unlike TGF-β1 that is predominantly involved in T cell-mediated immune tolerance (Batlle and Massague, 2019; Rubtsov and Rudensky, 2007), T cell-derived Activin-A promotes a pathogenic-Th17 cell response and exacerbates inflammation.

With multiple loss-of-function approaches, the current study highlighted an essential role for endogenous Activin-A for pathogenic-Th17 cell differentiation and autoimmunity. A recent study finds that administration of exogenous Activin-A attenuates autoimmunity with decreased Th17 cell pathogenicity and increased immune suppressive Treg cells (Morianos et al., 2020). These two studies collectively suggest that Activin-A controls T cell function in a dose and context dependent manner. On one hand, increased endogenous Activin-A in activated T cells under inflammatory conditions promotes pathogenic-Th17 cell differentiation through autocrine signaling. On the other hand, exogenous Activin-A may counter pathogenic-Th17 cell function and promote immune suppression via multiple mechanisms. These mechanisms may include (1) exogenous Activin-A tempering the pathogenicity of pathogenic-Th17 cells (Morianos et al., 2020) that produced high amounts of Activin-A as shown in this study, and (2) exogenous Activin-A enhancing the function of Treg cells (Morianos et al., 2020) that have high TGF-β1 activity (Green et al., 2003; Nakamura et al., 2001) because exogenous Activin-A can synergize with TGF-β1 to promote Treg cells (Huber et al., 2009). Further investigation is therefore warranted to understand how Activin-A regulates the intrinsic function of various T cell subsets and their cross-talks in a context and dose dependent manner during inflammation and autoimmunity.

Multiple mechanisms may contribute to the differential effects of Activin-A and TGF-β1 on pathogenic-Th17 cell function during autoimmunity. One could be that there is a difference in the responsiveness of T cells to Activin-A and TGF-β1 during activation and inflammation. We found that, in agreement with a previous report (Tu et al., 2018), TGF-β1-specific-receptor ALK5 was drastically decreased in $CD4^+$ T cells during inflammatory activation *in vitro* and *in vivo*, which made activated T cells much less sensitive to TGF-β1. In contrast, Activin-A-specific-receptor ALK4 was increased in $CD4^+$ T cells under the same inflammatory conditions and endowed activated T cells with sustained ability to differentiate into pathogenic-Th17 cells. Another mechanism could be that Activin-A-ALK4 and TGF-β1-ALK5 engage in different downstream pathways to diverge pathogenic- vs. non-pathogenic Th17 cell function. Indeed, we found that TGF-β1, but not Activin-A, induced a strong suppression of ERK activation. ERK phosphorylation was essential for the pathogenic function of Th17 cells because blockade of ERK phosphorylation inhibited pathogenic program but not Th17 cell differentiation. This observation connects the TGF-β1 pathway with ERK whose activation is known to be important for pathogenic-Th17 cell-driven autoimmunity (Brereton et al., 2009; Liu et al., 2013). We therefore propose a unified model as of how TGF-β1 controls the dichotomous function of pathogenic- and non-pathogenic-Th17 cells: while TGF-β1 promotes non-pathogenic-Th17 cells, it suppresses the pathogenic-Th17 cells through restraining ERK activity.

Activin-A is a cytokine expressed by different cell types to control multiple biological processes (Chen and Ten Dijke, 2016; Luisi et al., 2001; Morianos et al., 2019). We found that T cell-derived Activin-A was important for pathogenic-Th17 cell response. However

Author Manuscript Author Manuscript Author Manuscript Author Manuscript

there may also be non-T cell sources of Activin-A because ALK4-deficient T cells had slightly reduced ability than Activin-A-deficient T cells to differentiated into pathogenic-Th17 cells during EAE. T cell-produced Activin-A may also be involved in pathogenic-Th17 response during infection, because *Inhba* is expressed at much higher level in *Citrobacter rodentium*-induced inflammatory Th17 cells than in segmented filamentous bacteria (SFB) induced homeostatic Th17 cells (Omenetti et al., 2019). In addition, the insight gained from this study may also be relevant in humans, because *Inhba* is preferentially expressed in IL-23+IL-1β-differentiated human pathogenic-Th17 cells when compared to Th0 cells (Revu et al., 2018) and in IL-10^{-} Th17 cells when compared to IL-10^{+} Th17 cells (Aschenbrenner et al., 2018). Therefore, these findings may have broad implications in inflammation, infection, and autoimmunity in both mouse and human.

In summary, this study demonstrated a critical T cell-intrinsic role for Activin-A-ALK4-ERK in directing pathogenic-Th17 cell responses. It suggested that Activin-A, ALK4, and ERK may be promising therapeutic targets for treating pathogenic-Th17 cell related inflammatory diseases.

Limitations of the Study:

This study found increased Activin-A in the serums of human autoimmune disease patients with RRMS. Nonetheless, the cellular and anatomical origins of the Activin-A remain to be defined, as Activin-A can be produced by many different immune and non-immune cell types, especially under inflammatory conditions (Morianos et al., 2019; Werner and Alzheimer, 2006). Further assessment of Activin-A production in different immune and non-immune cell types in the CNS and the periphery would be needed in MS patients. In addition, although this study demonstrated a critical role for Activin-A-ALK4 axis in pathogenic-Th17 cell function in murine models, whether such a mechanism can be translated into human T cells warrants further study. Moreover, whereas this study showed that TGF-β1 inhibited ERK activation during pathogenic-Th17 cell differentiation, the precise underlying molecular and biochemical pathways remain to be elucidated. Furthermore, inflammatory stimuli including IL-6, IL-23, and IL-1β appeared to be the primary trigger to engage and synergize with Activin-A to promote pathogenic-Th17 cell response. It would be of interest to reveal how inflammatory cytokines promote Activin-A expression in T cells to identify ways to break the inflammation-Activin-A feed-forward mechanism to restrain pathogenic-Th17 cell function and suppress inflammatory diseases.

STAR ⋆ METHODS

RESOURCE AVAILABILITY

LEAD CONTACT—Further information and requests for resources and reagents should be directed to and will be fulfilled by the Lead Contact, Yisong Wan (wany@email.unc.edu).

MATERIALS AVAILABILITY—All unique/stable reagents generated in this study are available from the Lead Contact with a completed Materials Transfer Agreement.

Author Manuscript Author Manuscript Author Manuscript Author Manuscript

DATA AND CODE AVAILABILITY—RNA-seq data are deposited in GEO database under ID code: GSE151533.

EXPERIMENTAL MODEL AND SUBJECT DETAILS

Human subjects—Serum samples were obtained from untreated relapse remitting multiple sclerosis (RRMS) patients (n=22) in remission phase according to revised McDonald's diagnostic criteria (Thompson et al., 2018) and age-matched healthy controls (n=16). The age range of RRMS patients is 23–63 years. No statistical methods were used to predetermine sample size. On entering the study, subjects were in a stable condition and did not develop any clinical signs of infection for at least 4 weeks before evaluation. All Human participants signed an informed consent form and the study protocol was approved by the Institutional Review Board at Thomas Jefferson University. Detail information for all donors can be acquired upon request. The human serum samples were labled with simple numbers and the sample information was blinded to the investigators during ELISA assays. The sample information was not revealled until after data were analyzed.

Mice—*Cd4Cre*, $MOG_{35–55}$-specific 2D2 TCR-transgenic, and CD45.2 congenic mice were purchased from the Jackson Laboratory. *Cre*-dependent-*Cas9*-expressing were provided by Dr. Feng Zhang (Platt et al., 2014). CD45.1 congenic mice were purchased from Charles River. $CD45.1^+CD45.2^+$ mice were generated by breeding. All mice are on the C57BL/6 background. All mice were housed and bred in specific pathogen-free conditions in the animal facility at the University of North Carolina at Chapel Hill. All animal experiments were approved by the Institution Animal Care and Use Committee of the University of North Carolina. Gender and age-matched, 6–18 weeks old female and male mice were randomly assigned to experimental groups. Littermates were used if possible. Investigators were not blinded to animal experimental groups. No animal was excluded from analysis.

Cell culture—Primary mouse $CD4^+$ T cells from spleen and lymph nodes were isolated by mouse CD4 magnetic beads (Miltenyi Biotec) per manufacture's protocols. Isolated $CD4^+$ T cells were activated with 24 well-plate pre-coated with 10 μg/ml anti-CD3 (145–2C11, BioXCell) and 10 μg/ml anti-CD28 mAb (37.51, BioXCell) and cultured in serum-free X-VIVO 20 medium (Lonza) under various treatments as indicated in the method details and figure legends. The samples were labled with simple numbers during the experiments, without revealing the exact sample information until after data were analyzed. To generate recombinant viruses, HEK 293T cells (ATCC) were grown in DMEM (Gbico) + 10% FBS (Corning) + 1% penicillin-streptomycin (Gibco). All cells were cultured at 37°C in 5% CO_2-containing humidified incubators.

METHOD DETAILS

Flow-cytometry—Fluorescence-conjugated anti-GM-CSF (MP1–22E9), anti-IL-10 (JES5), anti-CD45.1 (A20), anti-CD45.2 (104), anti-CD4 (RM4–5), anti-Thy1.1 (OX-7), anti-IFN-γ (XMG1.2), and anti-IL17A (TC11–18H10.1) from Biolegend, as well as fluorescence-conjugated Annexin V and 7-amino-actinomycin D from BD Biosciences were used. For intracellular cytokine staining, lymphocytes were stimulated for 4 hours with 50 ng/ml of PMA (phorbol 12-myristate 13-acetate) and 1 μM ionomycin in the presence of 5

Author Manuscript Author Manuscript Author Manuscript Author Manuscript

μg /ml brefeldin A. Then 0.5–1×10^6 cells were fixed/permeabilized for 20 mins at 4 degree with Fixation/Permeabilization Solution Kit (BD Bioscience) and stained with fluorescently-conjugated antibodies per manufacture's protocols. For surface staning, 0.5–1×10^6 cells were collected and stained with fluorescently-conjugated antibodies for 15 mins at 4 degree. After wash, stained cells were recorded on Canto (BD Biosciences) and analyzed by FlowJo software (Treestar).

T cell activation, differentiation, and proliferation in vitro—1×10^6 $CD4^+$ T cells were isolated and activated in 24 well-plates pre-coated with 10 μg/ml anti-CD3 (145–2C11, BioXCell) and 10 μg/ml anti-CD28 mAb (37.51, BioXCell) in serum-free X-VIVO 20 medium (Lonza). For pathogenic-Th17 cell differentiation, 20 ng/ml IL-1β (Biolegend), 40 ng/ml IL-6 (Biolegend), 50 ng/ml IL-23 (Biolegend) and 20 μg/ml anti-IFN-γ (XMG1.2, BioXcell) were added to the culture. For TGF-β1+IL-6 induced Th17 cell differentiation, 1 ng/ml TGF-β1 (Biolegend), 40 ng/ml IL-6 (Biolegend) and 20 μg/ ml anti-IFN-γ (XMG1.2, BioXcell) were added to the culture. For Activin-A+IL-6 promoted Th17 cells, 30ng/ml Activin-A (Biolegend), 40 ng/ml IL-6 (Biolegend) and 20μg/ml anti-IFN-γ mAb (XMG1.2, BioXcell) were added to the culture. Anti-Activin-A (clone 69403, R&D), anti-TGF-β1 (1D11, BioXcell), Follistatin (R&D) and MEK inhibitor PD98059 (Selleckchem) were added when needed as indicated in the figure legends. To assess proliferation, isolated $CD4^+$ T Cells were labeled with 5 μM carboxyfluorescein diacetate succinimidyl ester (CFSE, AnaSpec) for 5 minutes at the room temperature. Labelled T cells were washed with PBS twice and activated under various conditions as indicated in the figure legends. The T cell proliferation was assessed 72 hours post activation based on CFSE dilution by flow-cytometry.

Active and passive transfer induced EAE in mice—For active EAE induction, 50μg murine myelin oligodendrocyte glycoprotein (MOG) peptide 35–55 (AnaSpec) in 100μl PBS was emulsified with 100μl complete Freund's adjuvant (CFA) that consists of incomplete Freund's adjuvant (Difco Laboratories) and 5mg/ml of *Mycobacterium tuberculosis* H37RA (Difco Laboratories). 200μl $MOG_{35–55}$+CFA was injected sub-cutaneously (s.c.) in both flanks of mice on day 0. 200ng Pertussis toxin (List Biological) in 200μl PBS was injected intra-peritoneally (i.p.) on day 0 and day 2.

For passive transfer induced EAE, 2D2 T cells were differentiated under various conditions as indicated in the figures and figure legends, and re-stimulated in 24 well-plates pre-coated with 2 μg/ml anti-CD3 and 2 μg/ml anti-CD28 mAb in fresh medium for 2 days. 1×10^6 live cells were purified and i.v injected into 400 cGy-irradiated recipient mice in 200μl PBS. 200ng Pertussis toxin (List Biological)) in 200μl PBS was injected i.p. on day 0 and day 2 after T cell transfer.

The severity of EAE was monitored for clinical scores from 0 to 5: 0 = No clinical signs; 1 = Limp tail; 2 = Para-paresis (weakness, incomplete paralysis of one or two hind limbs); 3 = Paraplegia (complete paralysis of two hind limbs); 4 = Paraplegia with forelimb weakness or paralysis; 5 = Moribund or death.

Author Manuscript Author Manuscript Author Manuscript Author Manuscript

After EAE induction, diseased and non-diseased mice were sacrificed and perfused with ice-cold phosphate buffered saline containing 20 U/ml heparin. Spinal cords were separated from spinal columns after removal of all tissues. Isolated spinal cords were dissected and digested with 1 mg/ml collagenase D (Sigma) for 45 minutes at 37°C water bath. The digested tissue was then centrifuged in 38% percoll (Sigma) at 2,000 rpm for 20 minutes to separate mononuclear cells. Residual red blood cells were lysed by Ammonium-Chloride-Potassium (ACK) Lysing Buffer. The lymphocytes were then washed with PBS and subjected for subsequent analysis.

Quantitative RT-PCR (qRT-PCR) and RNA-seq analysis—For qRT-PCR analysis, total RNA was extracted from T cells using TRizol reagent (Invitrogen) and reverse-transcribed into cDNA using iScriptTM cDNA Synthesis Kit (Bio-Rad) per manufacturer's protocols. Quantitative PCR (qPCR) was then performed using iTaq Universal Probes Supermix (Bio-rad) and selected probes (Integrated DNA Technologies) on QuantStudio® 6 Flex Real-Time PCR System (ThermoFisher Scientific). The relative mRNA amounts of genes of interest to endogenous control β-actin were presented using arbitrary units.

For RNA-seq analysis, total RNA was extracted from T cells by using Direct-zol RNA Miniprep (ZYMO Research). RNA-seq libraries were sequenced using the 100-bp paired-end mode via the DNBseq (BGI) according to the manufacturer's protocol. The raw reads were filtered by removing adaptor sequences, contamination, and low-quality reads. Cleaned reads (~20 million reads sample) were aligned to the mm10 reference genome using STAR (Version 2.5.1). The quantification results from "featureCount (subread, Version 1.4.6)" were then analyzed with the Bioconductor package DESeq2, which fits a negative binomial distribution to estimate technical and biological variability. PCA plot was generated to identify sample outlier (Partek Version 7.2, CA, USA). Differential expression genes (DEG) were identified and a gene was considered differentially expressed when the p value was less than 0.05. Visualization of DEG was performed with heatmap library in R (Version 3.6.3). Potential enrichment of pathogenic and nonpathogenic gene sets and IL-10 related programs were further analyzed with Broad Institute's GSEA tool (Version 4.0.3).

Immuno-blotting analysis—Protein was extracted by RIPA lysis buffer (Sigma) and resolved in Any kD™ Mini-PROTEAN® TGX™ Precast Protein Gels (Bio-Rad), transferred to a polyvinylidene fluoride membrane (Bio-Rad) and blocked with 5% BSA at room temprature for 1 hour and analyzed by immuno-blotting with the following antibodies: anti-SKI (G8, Santa Cruz), anti-ALK4 (EPR4815, Abcam), anti-ALK5 (Abcam), anti-p-Smad2 (S465/467) (138D4, CST), anti-Smad2 (D43B4, CST), anti-p-ERK1/2 (Thr202/Tyr204) (CST), anti-ERK1/2 (clone 16, BD), anti-p-STAT3 (Tyr705) (3E2, CST), anti-STAT3 (124H6, CST), and anti-β-actin antibodies (I-19, Santa Cruz), at 4°C overnight. The blot was subsequently incubated with horseradish peroxidase-linked secondary antibodies (Santa Cruz) at room temprature for 1 hour and the signal was detected using SuperSignal™ West Pico PLUS Chemilum inescent Substrate (Thermofisher). The relative protein amounts of SKI, ALK4, ALK5 to endogenous control β-actin, p-Smad2 to Smad2, and p-ERK1/2 to ERK1/2 were quantified by densitometric analysis using Image J software (Schneider et al., 2012) and presented using arbitrary units.

Author Manuscript Author Manuscript Author Manuscript Author Manuscript

ELISA—Blood samples from all human subjects were collected in BD vacutainer sodium heparin tubes. All samples are kept on bench overnight and serum samples were collected next morning after centrifugation at 5,000 rpm for 5 mins. The supernatant of spinal cord homogenates and serum from EAE mice were collected at day 14–16 post disease elicitation. Activin-A protein amounts were measured in human serum samples, mouse serum and the supernatant of spinal cord homogenates, and in mouse Th17 cell culture supernatants by a Activin-A ELISA Kit (R&D, Cata#DAC00B) per manufacture's protocols.

Ectopic gene expression and shRNA-mediated RNAi—For ectopic gene expression, full-length cDNA encoding *Fst* (Transomics, Cat# BC145945) was cloned into MSCV-IRES-Thy1.1 (RV) vector (Addgene #17442) (Wu et al., 2006). In addition, constitutively activated form of ALK4 (ca-ALK4) and ALK5 (ca-ALK5) were constructed by creating T206D and T204D mutants respectively from cDNA of wild-type ALK4 (Clone ID:40131078, Dharmacon) and ALK5 (Clone ID:6409765, Dharmacon) and cloned into MSCV-IRES-Thy1.1 (RV) vector.

For shRNA-mediated RNAi, lenti-viral shRNA constructs carrying puromycin resistance genes were purchased from shRNA core facility at UNC Chapel Hill. Scrambled shRNA constructs (pLKO.1-scramble shRNA control) carrying puromycin resistance gene was obtained from Addgene (Moffat et al., 2006).

To produce recombinant viruses, HEK293T cells were grown to a confluency of 80–90% for transfecton. For lentivirus production, lenti-viral shRNA construts, pMD2.G (Addgene #12259, a gift from Didier Trono) and psPAX2 (Addgene #12260, a gift from Didier Trono) were tranfected at a 10:5:9 ratio in HEK293T cells using FuGENE (Promega) per manufacture's instruction. For retrovirus production, retroviral constructs were transfected with pCL-Eco (Addgene#12371) (Naviaux et al., 1996) at a 3:1 ratio in HEK293T cells using FuGENE (Promega) per manufacture's instruction. Viruses were collected at day 2–3 after transfection and stored at −80°C.

For retroviral and lentiviral transduction, $CD4^+$ T cells were isolated and cultured under various conditions as described in the figures and figure legends, and then spin-inoculated at 1,500 × g with indicated recombinant virus in the presence of 8 μg/ml polybrene (Sigma-Aldrich) and 10 mM HEPES buffer (Gibco) at 30 °C for 90 min, 24 hr post activation. Transduced cells were harvested and analyzed at indicated time. Antibiotic selection was performed, when applicable, by adding 2 μg/ml puromycin in the culture medium for 4 days. The transduced cells were selected based on puromycin resistance.

Activin-A and ALK4 guide RNA design for CRISPR/Cas9—Guide RNAs (gRNAs) targeting Activin-A and ALK4 were designed by the CHOPCHOP web tool (https://chopchop.cbu.uib.no/). gRNAs of the highest score and specificity were selected based on the algorithm. The sequences for the chosen gRNAs were Activin-A gRNA: ACCCCAGGATCCGAGGGGCA and ALK4 gRNA: GTTACTATGGCGGAGTCGGC. gRNAs were then cloned into lentis-U6-sgRNA-SFFV-Cas9-Thy1.1 vector. sgRNA expressing viruses were produced in HEK293T cells and transduced into activated $CD4^+$ T cells.

Author Manuscript Author Manuscript Author Manuscript Author Manuscript

QUANTIFICATION AND STATISTICAL ANALYSIS

Statistical analysis of results was performed using GraphPad Prism (Version 7, GraphPad software). No statistical method was used to predetermine the sample size. All collected data are analyzed without exclusion. Two-sided Student's *t*-test was used to compare two groups of samples. Two-way multiple-range ANOVA test was used to compare multiple groups of samples in EAE experiments. $p<0.05$ (confidence interval of 95%) was considered statistically significant. In the figures, *, **, *** and **** were used to indicate $p<0.05$, $p<0.01$, $p<0.001$ and $p<0.0001$, respectively. Figure legends specified the tests used, statistical significance, and the numbers of experimental and biological replicates.

Supplementary Material

Refer to Web version on PubMed Central for supplementary material.

Acknowledgement:

We thank F. Zhang for *Cre*-dependent-*Cas9*-expressing mice and J. McGuire for the clinical data. We also thank the supports from the Intramural Research Program of the NIEHS for J.L, and NIH/NIAID (AI123193), National Multiple Sclerosis Society (RG4654), and Yang Family Biomedical Scholars Award for Y.Y.W.

References

Aschenbrenner D, Foglierini M, Jarrossay D, Hu D, Weiner HL, Kuchroo VK, Lanzavecchia A, Notarbartolo S, and Sallusto F (2018). An immunoregulatory and tissue-residency program modulated by c-MAF in human TH17 cells. Nat Immunol 19, 1126–1136. [PubMed: 30201991]

Batlle E, and Massague J (2019). Transforming Growth Factor-beta Signaling in Immunity and Cancer. Immunity 50, 924–940. [PubMed: 30995507]

Bauer J, Ozden O, Akagi N, Carroll T, Principe DR, Staudacher JJ, Spehlmann ME, Eckmann L, Grippo PJ, and Jung B (2015). Activin and TGFbeta use diverging mitogenic signaling in advanced colon cancer. Mol Cancer 14, 182. [PubMed: 26497569]

Bettelli E, Carrier Y, Gao W, Korn T, Strom TB, Oukka M, Weiner HL, and Kuchroo VK (2006). Reciprocal developmental pathways for the generation of pathogenic effector TH17 and regulatory T cells. Nature 441, 235–238. [PubMed: 16648838]

Brereton CF, Sutton CE, Lalor SJ, Lavelle EC, and Mills KH (2009). Inhibition of ERK MAPK suppresses IL-23- and IL-1-driven IL-17 production and attenuates autoimmune disease. Journal of immunology 183, 1715–1723.

Chen W, and Ten Dijke P (2016). Immunoregulation by members of the TGFbeta superfamily. Nature reviews. Immunology 16, 723–740.

David CJ, and Massague J (2018). Contextual determinants of TGFbeta action in development, immunity and cancer. Nature reviews. Molecular cell biology 19, 419–435. [PubMed: 29643418]

de Kretser DM, O'Hehir RE, Hardy CL, and Hedger MP (2012). The roles of activin A and its binding protein, follistatin, in inflammation and tissue repair. Mol Cell Endocrinol 359, 101–106. [PubMed: 22037168]

Derynck R, and Budi EH (2019). Specificity, versatility, and control of TGF-beta family signaling. Sci Signal 12.

Dong C (2006). Diversification of T-helper-cell lineages: finding the family root of IL-17-producing cells. Nature reviews. Immunology 6, 329–333.

Esplugues E, Huber S, Gagliani N, Hauser AE, Town T, Wan YY, O'Connor W Jr., Rongvaux A, Van Rooijen N, Haberman AM, et al. (2011). Control of TH17 cells occurs in the small intestine. Nature 475, 514–518. [PubMed: 21765430]

Author Manuscript Author Manuscript Author Manuscript Author Manuscript

Gaublomme JT, Yosef N, Lee Y, Gertner RS, Yang LV, Wu C, Pandolfi PP, Mak T, Satija R, Shalek AK, et al. (2015). Single-Cell Genomics Unveils Critical Regulators of Th17 Cell Pathogenicity. Cell 163, 1400–1412. [PubMed: 26607794]

Ghoreschi K, Laurence A, Yang XP, Hirahara K, and O'Shea JJ (2011). T helper 17 cell heterogeneity and pathogenicity in autoimmune disease. Trends in immunology 32, 395–401. [PubMed: 21782512]

Ghoreschi K, Laurence A, Yang XP, Tato CM, McGeachy MJ, Konkel JE, Ramos HL, Wei L, Davidson TS, Bouladoux N, et al. (2010). Generation of pathogenic T(H)17 cells in the absence of TGF-beta signalling. Nature 467, 967–971. [PubMed: 20962846]

Green EA, Gorelik L, McGregor CM, Tran EH, and Flavell RA (2003). CD4+CD25+ T regulatory cells control anti-islet CD8+ T cells through TGF-beta-TGF-beta receptor interactions in type 1 diabetes. Proceedings of the National Academy of Sciences of the United States of America 100, 10878–10883. [PubMed: 12949259]

Gutcher I, Donkor MK, Ma Q, Rudensky AY, Flavell RA, and Li MO (2011). Autocrine transforming growth factor-beta1 promotes in vivo Th17 cell differentiation. Immunity 34, 396–408. [PubMed: 21435587]

Harrison CA, Gray PC, Vale WW, and Robertson DM (2005). Antagonists of activin signaling: mechanisms and potential biological applications. Trends Endocrinol Metab 16, 73–78. [PubMed: 15734148]

Hedger MP, and de Kretser DM (2013). The activins and their binding protein, follistatin-Diagnostic and therapeutic targets in inflammatory disease and fibrosis. Cytokine Growth Factor Rev 24, 285–295. [PubMed: 23541927]

Heldin CH, and Moustakas A (2016). Signaling Receptors for TGF-beta Family Members. Cold Spring Harb Perspect Biol 8.

Huber S, Stahl FR, Schrader J, Luth S, Presser K, Carambia A, Flavell RA, Werner S, Blessing M, Herkel J, and Schramm C (2009). Activin a promotes the TGF-beta-induced conversion of CD4+CD25- T cells into Foxp3+ induced regulatory T cells. Journal of immunology 182, 4633–4640.

Jones CP, Gregory LG, Causton B, Campbell GA, and Lloyd CM (2012). Activin A and TGF-beta promote T(H)9 cell-mediated pulmonary allergic pathology. The Journal of allergy and clinical immunology 129, 1000–1010 e1003. [PubMed: 22277204]

Korn T, Bettelli E, Oukka M, and Kuchroo VK (2009). IL-17 and Th17 Cells. Annual review of immunology 27, 485–517.

Lee JY, Hall JA, Kroehling L, Wu L, Najar T, Nguyen HH, Lin WY, Yeung ST, Silva HM, Li D, et al. (2020). Serum Amyloid A Proteins Induce Pathogenic Th17 Cells and Promote Inflammatory Disease. Cell 180, 79–91 e16. [PubMed: 31866067]

Lee Y, Awasthi A, Yosef N, Quintana FJ, Xiao S, Peters A, Wu C, Kleinewietfeld M, Kunder S, Hafler DA, et al. (2012). Induction and molecular signature of pathogenic TH17 cells. Nature immunology 13, 991–999. [PubMed: 22961052]

Li MO, Wan YY, and Flavell RA (2007). T cell-produced transforming growth factor-beta1 controls T cell tolerance and regulates Th1- and Th17-cell differentiation. Immunity 26, 579–591. [PubMed: 17481928]

Liu H, Yao S, Dann SM, Qin H, Elson CO, and Cong Y (2013). ERK differentially regulates Th17- and Treg-cell development and contributes to the pathogenesis of colitis. European journal of immunology 43, 1716–1726. [PubMed: 23620016]

Locci M, Wu JE, Arumemi F, Mikulski Z, Dahlberg C, Miller AT, and Crotty S (2016). Activin A programs the differentiation of human TFH cells. Nature immunology 17, 976–984. [PubMed: 27376469]

Luisi S, Florio P, Reis FM, and Petraglia F (2001). Expression and secretion of activin A: possible physiological and clinical implications. Eur J Endocrinol 145, 225–236. [PubMed: 11517001]

Mangan PR, Harrington LE, O'Quinn DB, Helms WS, Bullard DC, Elson CO, Hatton RD, Wahl SM, Schoeb TR, and Weaver CT (2006). Transforming growth factor-beta induces development of the T(H)17 lineage. Nature 441, 231–234. [PubMed: 16648837]

Author Manuscript Author Manuscript Author Manuscript Author Manuscript

Martinez GJ, Zhang Z, Reynolds JM, Tanaka S, Chung Y, Liu T, Robertson E, Lin X, Feng XH, and Dong C (2010). Smad2 positively regulates the generation of Th17 cells. The Journal of biological chemistry 285, 29039–29043. [PubMed: 20667820]

McGeachy MJ, Bak-Jensen KS, Chen Y, Tato CM, Blumenschein W, McClanahan T, and Cua DJ (2007). TGF-beta and IL-6 drive the production of IL-17 and IL-10 by T cells and restrain T(H)-17 cell-mediated pathology. Nat Immunol 8, 1390–1397. [PubMed: 17994024]

Moffat J, Grueneberg DA, Yang X, Kim SY, Kloepfer AM, Hinkle G, Piqani B, Eisenhaure TM, Luo B, Grenier JK, et al. (2006). A lentiviral RNAi library for human and mouse genes applied to an arrayed viral high-content screen. Cell 124, 1283–1298. [PubMed: 16564017]

Moren A, Imamura T, Miyazono K, Heldin CH, and Moustakas A (2005). Degradation of the tumor suppressor Smad4 by WW and HECT domain ubiquitin ligases. The Journal of biological chemistry 280, 22115–22123. [PubMed: 15817471]

Morianos I, Papadopoulou G, Semitekolou M, and Xanthou G (2019). Activin-A in the regulation of immunity in health and disease. J Autoimmun, 102314. [PubMed: 31416681]

Morianos I, Trochoutsou AI, Papadopoulou G, Semitekolou M, Banos A, Konstantopoulos D, Manousopoulou A, Kapasa M, Wei P, Lomenick B, et al. (2020). Activin-A limits Th17 pathogenicity and autoimmune neuroinflammation via CD39 and CD73 ectonucleotidases and Hif1-alpha-dependent pathways. Proceedings of the National Academy of Sciences of the United States of America 117, 12269–12280. [PubMed: 32409602]

Moustakas A, and Heldin CH (2005). Non-Smad TGF-beta signals. J Cell Sci 118, 3573–3584. [PubMed: 16105881]

Nakamura K, Kitani A, and Strober W (2001). Cell contact-dependent immunosuppression by CD4(+)CD25(+) regulatory T cells is mediated by cell surface-bound transforming growth factor beta. The Journal of experimental medicine 194, 629–644. [PubMed: 11535631]

Naviaux RK, Costanzi E, Haas M, and Verma IM (1996). The pCL vector system: rapid production of helper-free, high-titer, recombinant retroviruses. Journal of virology 70, 5701–5705. [PubMed: 8764092]

Ogawa K, Funaba M, Chen Y, and Tsujimoto M (2006). Activin A functions as a Th2 cytokine in the promotion of the alternative activation of macrophages. Journal of immunology 177, 6787–6794.

Omenetti S, Bussi C, Metidji A, Iseppon A, Lee S, Tolaini M, Li Y, Kelly G, Chakravarty P, Shoaie S, et al. (2019). The Intestine Harbors Functionally Distinct Homeostatic Tissue-Resident and Inflammatory Th17 Cells. Immunity.

Phillips DJ, de Kretser DM, and Hedger MP (2009). Activin and related proteins in inflammation: not just interested bystanders. Cytokine Growth Factor Rev 20, 153–164. [PubMed: 19261538]

Platt RJ, Chen S, Zhou Y, Yim MJ, Swiech L, Kempton HR, Dahlman JE, Parnas O, Eisenhaure TM, Jovanovic M, et al. (2014). CRISPR-Cas9 knockin mice for genome editing and cancer modeling. Cell 159, 440–455. [PubMed: 25263330]

Revu S, Wu J, Henkel M, Rittenhouse N, Menk A, Delgoffe GM, Poholek AC, and McGeachy MJ (2018). IL-23 and IL-1beta Drive Human Th17 Cell Differentiation and Metabolic Reprogramming in Absence of CD28 Costimulation. Cell reports 22, 2642–2653. [PubMed: 29514093]

Rubtsov YP, and Rudensky AY (2007). TGFbeta signalling in control of T-cell-mediated self-reactivity. Nature reviews. Immunology 7, 443–453.

Schneider CA, Rasband WS, and Eliceiri KW (2012). NIH Image to ImageJ: 25 years of image analysis. Nat Methods 9, 671–675. [PubMed: 22930834]

Sideras P, Apostolou E, Stavropoulos A, Sountoulidis A, Gavriil A, Apostolidou A, and Andreakos E (2013). Activin, neutrophils, and inflammation: just coincidence? Semin Immunopathol 35, 481–499. [PubMed: 23385857]

Stockinger B, and Omenetti S (2017). The dichotomous nature of T helper 17 cells. Nat Rev Immunol 17, 535–544. [PubMed: 28555673]

ten Dijke P, Yamashita H, Ichijo H, Franzen P, Laiho M, Miyazono K, and Heldin CH (1994). Characterization of type I receptors for transforming growth factor-beta and activin. Science 264, 101–104. [PubMed: 8140412]

Author Manuscript Author Manuscript Author Manuscript Author Manuscript

Thompson AJ, Banwell BL, Barkhof F, Carroll WM, Coetzee T, Comi G, Correale J, Fazekas F, Filippi M, Freedman MS, et al. (2018). Diagnosis of multiple sclerosis: 2017 revisions of the McDonald criteria. Lancet Neurol 17, 162–173. [PubMed: 29275977]

Tsuchida K, Nakatani M, Hitachi K, Uezumi A, Sunada Y, Ageta H, and Inokuchi K (2009). Activin signaling as an emerging target for therapeutic interventions. Cell Commun Signal 7, 15. [PubMed: 19538713]

Tu E, Chia CPZ, Chen W, Zhang D, Park SA, Jin W, Wang D, Alegre ML, Zhang YE, Sun L, and Chen W (2018). T Cell Receptor-Regulated TGF-beta Type I Receptor Expression Determines T Cell Quiescence and Activation. Immunity 48, 745–759 e746. [PubMed: 29669252]

Veldhoen M, Hocking RJ, Atkins CJ, Locksley RM, and Stockinger B (2006). TGFbeta in the context of an inflammatory cytokine milieu supports de novo differentiation of IL-17-producing T cells. Immunity 24, 179–189. [PubMed: 16473830]

Wang C, Yosef N, Gaublomme J, Wu C, Lee Y, Clish CB, Kaminski J, Xiao S, Meyer Zu Horste G, Pawlak M, et al. (2015). CD5L/AIM Regulates Lipid Biosynthesis and Restrains Th17 Cell Pathogenicity. Cell 163, 1413–1427. [PubMed: 26607793]

Wang X, Ni L, Wan S, Zhao X, Ding X, Dejean A, and Dong C (2020). Febrile Temperature Critically Controls the Differentiation and Pathogenicity of T Helper 17 Cells. Immunity 52, 328–341 e325. [PubMed: 32049050]

Weaver CT, Harrington LE, Mangan PR, Gavrieli M, and Murphy KM (2006). Th17: an effector CD4 T cell lineage with regulatory T cell ties. Immunity 24, 677–688. [PubMed: 16782025]

Weiss A, and Attisano L (2013). The TGFbeta superfamily signaling pathway. Wiley Interdiscip Rev Dev Biol 2, 47–63. [PubMed: 23799630]

Werner S, and Alzheimer C (2006). Roles of activin in tissue repair, fibrosis, and inflammatory disease. Cytokine & growth factor reviews 17, 157–171. [PubMed: 16481210]

Wu Y, Borde M, Heissmeyer V, Feuerer M, Lapan AD, Stroud JC, Bates DL, Guo L, Han A, Ziegler SF, et al. (2006). FOXP3 controls regulatory T cell function through cooperation with NFAT. Cell 126, 375–387. [PubMed: 16873067]

Zhang S, Takaku M, Zou L, Gu AD, Chou WC, Zhang G, Wu B, Kong Q, Thomas SY, Serody JS, et al. (2017). Reversing SKI-SMAD4-mediated suppression is essential for TH17 cell differentiation. Nature 551, 105–109. [PubMed: 29072299]

Author Manuscript Author Manuscript Author Manuscript Author Manuscript

Highlights

1. Activin-A expression is induced in T cells in autoimmunity and inflammation.
2. Autocrine Activin-A-ALK4 signal is essential for pathogenic-Th17 cell response.
3. Activin-A+IL-6 promotes pathogenic Th17 cell differentiation.
4. Activin-A permits ERK activation to endow Th17 cells with pathogenic function.

Author Manuscript Author Manuscript Author Manuscript Author Manuscript

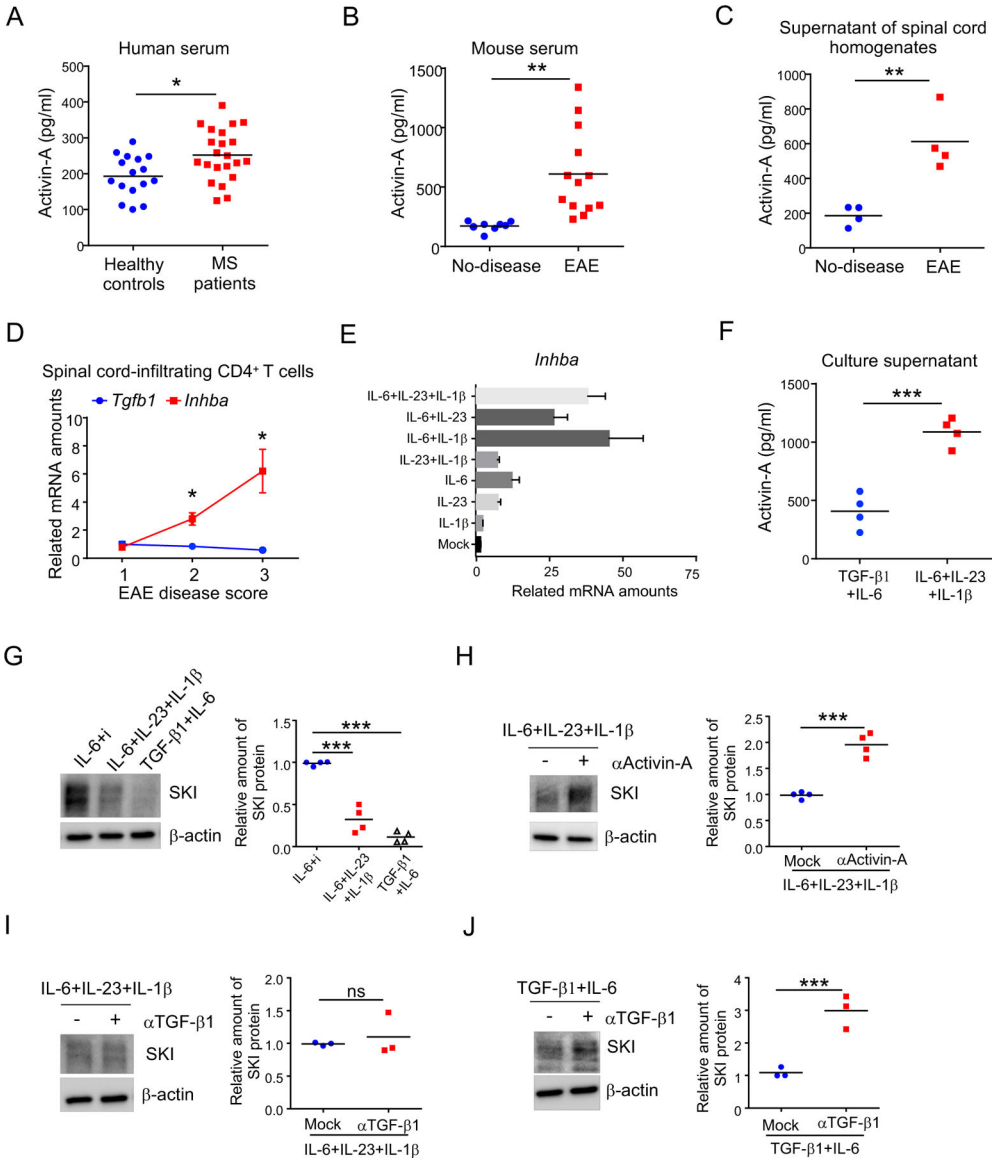

Figure 1. Activin-A protein level was increased under inflammatory condition *in vivo* and *in vitro*.

See also Figure S1.

(**A**) Activin-A protein levels in the sera of 22 recently diagnosed untreated RRMS patients and 16 healthy controls (HCs), assayed by ELISA. (*p<0.05, two-sided *t*-test; center bars indicate mean values)

(**B–C**) Activin-A protein levels in the sera (**B**) and the supernatant of spinal cord homogenates (**C**) from mice with EAE, assayed by ELISA. (n=8–13 samples from 3 independent experiments for **B**, n=4 samples from 3 independent experiments for **C**; **p<0.01, two-sided *t*-test; center bars indicate mean values)

(**D**) mRNA expression of Activin-A (*Inhba*) and TGF-β1 (*Tgfb1*) in $CD4^+$ T cells infiltrating spinal cords of mice with EAE with indicated clinical scores, assayed by qRT-PCR. (n=4 mice for each group from 3 experiments; mean ± s.d., *p<0.05, two-sided *t*-test)

Author Manuscript Author Manuscript Author Manuscript Author Manuscript

(**E**) mRNA expression of Activin-A (*Inhba*) in $CD4^+$ T cells activated under indicated conditions for 2 days, assayed by qRT-PCR. (n=3 samples from 3 experiments; mean ± s.d.)
(**F**) Activin-A protein levels in the supernatants of $CD4^+$ T cells activated in the presence of IL-6+IL-23+IL-1β and TGF-β1+IL-6 for 4 days, assayed by ELISA (n=4 samples from 4 experiments; ***p<0.001, two-sided *t*-test; center bars indicate mean values)
(**G**) Immuno-blotting to detect SKI protein expression in $CD4^+$ T cells activated in the presence of IL-6+TGFβRI inhibitor (i), IL-6+IL-23+IL-1β, or TGF-β1+IL-6, for 2 days. The relative SKI protein amount was determined by densitometry. (n=4 experiments; ***p<0.001, two-sided *t*-test; center bars indicate mean values)
(**H**) Immuno-blotting to detect SKI protein expression in $CD4^+$ T cells activated in the presence of IL-6+IL-23+IL-1β for 2 days, with (+) or without (−) Activin-A-neutralizing antibody (2 μg/ml αActivin-A). The relative SKI protein amount was determined by densitometry. (n=4 experiments; ***p<0.001, two-sided *t*-test; center bars indicate mean values)
(**I–J**) Immuno-blotting to detect SKI protein expression in $CD4^+$ T cells activated in the presence of IL-6+IL-23+IL-1β (**I**) and TGF-β1+IL-6 (**J**) for 2 days, with (+) or without (−) TGF-β1-neutralizing antibody (10 μg/ml αTGF-β1). The relative SKI protein amount was determined by densitometry. (n=3 experiments; ns, not significant, ***p<0.001, two-sided *t*-test; center bars indicate mean values)

Author Manuscript Author Manuscript Author Manuscript Author Manuscript

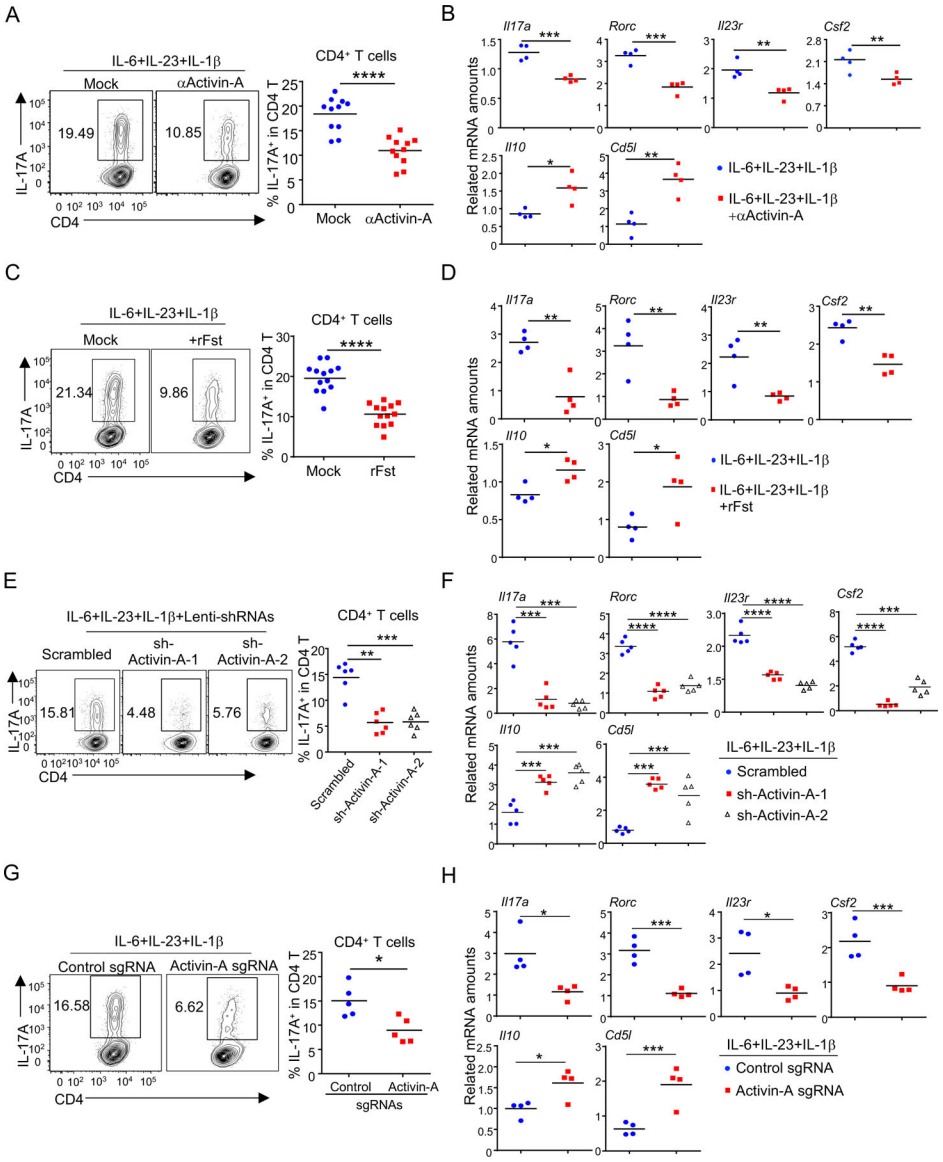

Figure 2. Activin-A was critical for pathogenic-Th17 cell differentiation *in vitro*.

See also Figure S2.

(**A**) IL-17A production by CD4$^+$ T cells activated in the presence of IL-6+IL-23+IL-1β for 4 days, with 2 μg/ml αActivin-A or without (Mock), assayed by flow-cytometry. (n=11 samples from 5 experiments; ****p<0.0001, two-sided *t*-test; center bars indicate mean values)

(**B**) mRNA expression of Th17-related genes in CD4$^+$ T cells as in **A**, assayed by qRT-PCR. (n=4 samples from 4 experiments; *p<0.01, **p<0.01, ***p<0.001, two-sided *t*-test; center bars indicate mean values)

(**C**) IL-17A production by CD4$^+$ T cells activated in the presence of IL-6+IL-23+IL-1β for 4 days, with 100 ng/ml recombinant Follistatin (rFst) or without (Mock), assayed by flow-cytometry. (n=13 samples from 4 experiments; ****p<0.001, two-sided *t*-test; center bars indicate mean values)

Author Manuscript Author Manuscript Author Manuscript Author Manuscript

(**D**) mRNA expression of Th17-related genes in $CD4^+$ T cells as in **C**, assayed by qRT-PCR (n=4 samples from 4 experiments; *p<0.01, **p<0.01, two-sided *t*-test; center bars indicate mean values)

(**E**) IL-17A production by $CD4^+$ T cells activated in the presence of IL-6+IL-23+IL-1β and transduced by lentivirus expressing Activin-A shRNAs (sh-Activin-A) or scrambled shRNA for 4 days, assayed by flow-cytometry. (n=6 samples from 3 experiments; **p<0.01, ***p<0.001, two-sided *t*-test; center bars indicate mean values)

(**F**) mRNA expression of Th17-related genes in $CD4^+$ T cells as in **E**, assayed by qRT-PCR. (n=5 samples from 3 experiments; ***p<0.001, ****p<0.0001, two-sided *t*-test; center bars indicate mean values)

(**G**) $CD4^+$ T cells from *CD4cre*-dependent-*Cas9*-expressing mice were activated in the presence of IL-6+IL-23+IL-1β and transduced with lentivirus expressing Activin-A sgRNA or control sgRNA. $IL\text{-}17A^+$ cells were detected 4 days after transduction by flow-cytometry. (n=5 samples from 3 experiments; *p<0.05, two-sided *t*-test; center bars indicate mean values)

(**H**) mRNA expression of Th17-related genes in $CD4^+$ T cells as in **G**, assayed by qRT-PCR. (n=4 samples from 3 experiments; *p<0.05, ***p<0.001, two-sided *t*-test; center bars indicate mean values)

Author Manuscript Author Manuscript Author Manuscript Author Manuscript

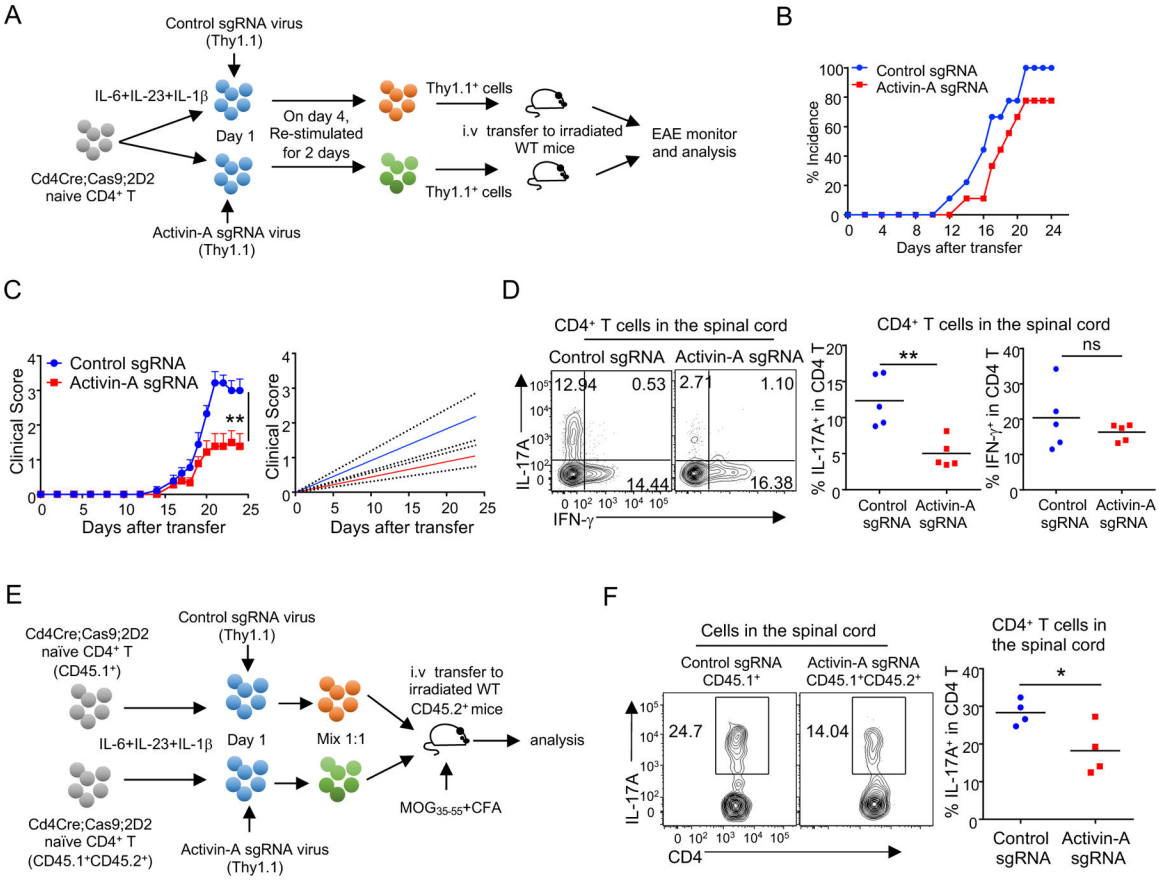

Figure 3. Activin-A was required for pathogenic-Th17 cell mediated neuroinflammation.

(**A**) Schema of adoptive transfer of 2D2 T cells to elicit EAE disease. CD4$^+$ T cells from *Cd4Cre;Cas9;2D2* mice were activated in the presence of IL-6+IL-23+IL-1β and transduced with lentivirus expressing Activin-A sgRNA or control sgRNA together with Thy1.1. T cells were re-stimulated for 2 days without cytokines. 1×10^6 transduced (Thy1.1$^+$) T cells were purified and i.v injected to 400 cGy irradiated recipient mice to elicit EAE.

(**B–C**) The comparison of the EAE incidence (**B**), clinical scores (**C**, left panel), and the linear-regression analysis (**C**, right panel) of the mice received different T cells depicted in **A**. (n=9 mice in each group from three experiments; mean ± s.e.m., **p<0.01, two-way multiple-range ANOVA test)

(**D**) IL-17A- and IFN-γ production by Thy1.1$^+$CD4$^+$ T cells infiltrating in the spinal cords of mice with EAE as in **A-C**, assayed by flow-cytometry. (n=5 samples from 3 experiments; ns, not significant, **p<0.01, two-sided *t*-test; center bars indicate mean values)

(**E**) Schema of adoptive transfer of both control sgRNA transduced T cells (CD45.1$^+$) and Activin-A sgRNA transduced T cells (CD45.1$^+$CD45.2$^+$) into irradiated recipient mice (CD45.2$^+$), where EAE was elicited with $MOG_{35–55}$+CFA.

(**F**) IL-17A production by sgRNA virus transduced (Thy1.1$^+$) CD4$^+$ T cells infiltrating in the spinal cords of EAE-inflicted recipient mice as described in **E**, assayed by flow-cytometry (n=4 samples from 3 experiments; *p<0.05, two-sided *t*-test; center bars indicate mean values)

Author Manuscript Author Manuscript Author Manuscript Author Manuscript

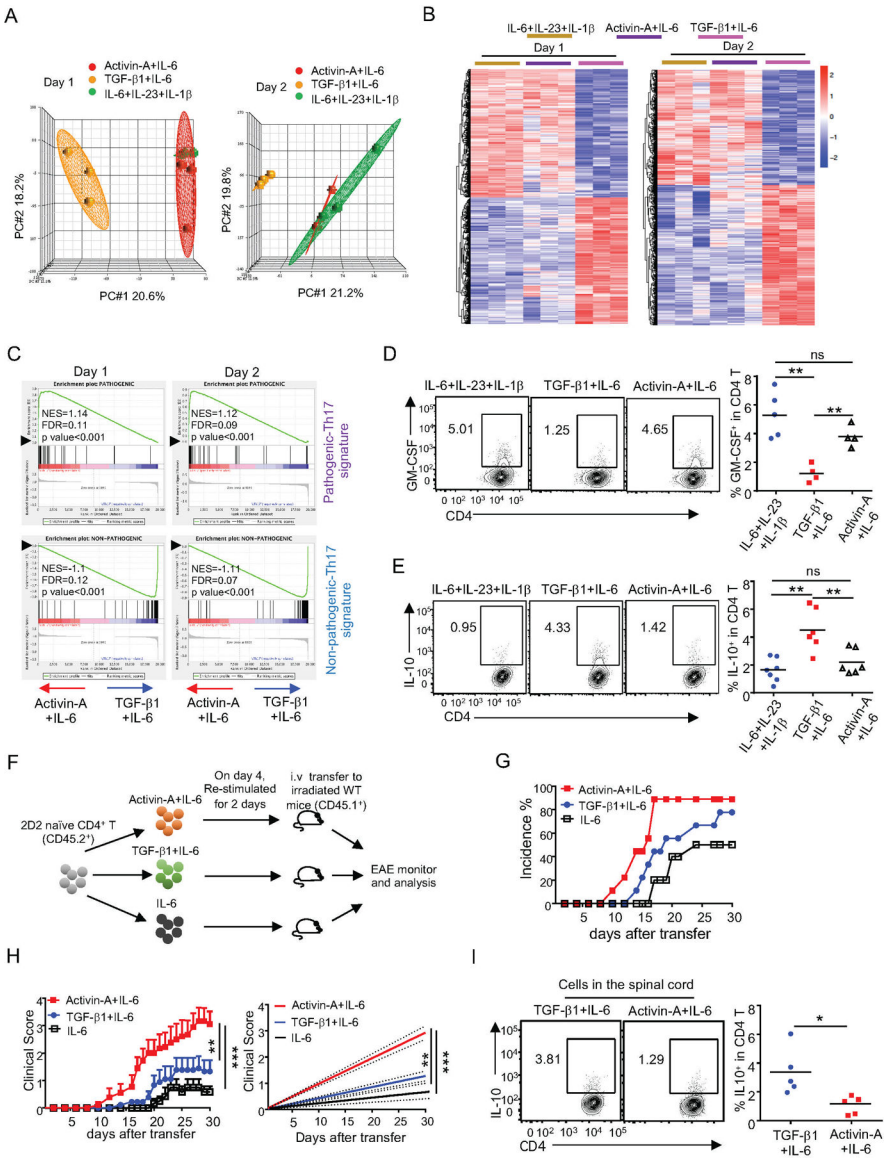

Figure 4. Activin-A induced pathogenic Th17 cells in the presence of IL-6.

See also Figure S3.

(**A**) PCA analysis of genome-wide gene expression of $CD4^+$ T cells activated for 1 and 2 days in the presence of indicated cytokine combinations. (Results combined 3 samples from 3 experiments)

(**B**) Heatmap and cluster analysis of differentially expressed genes (IL-6+IL-23+IL-1β vs TGF-β1+IL-6) in $CD4^+$ T cells activated in the presence of IL-6+IL-23+IL-1β, Activin-A +IL-6, or TGF-β1+IL-6 for 1 day and 2 days. Adjusted p value<0.05 was used as cutoff.

(**C**) Gene set enrichment analysis (GSEA) of pathogenic-Th17 gene set in Activin-A+IL-6-driven Th17 cells and non-pathogenic-Th17 gene set in TGF-β1+IL-6-driven Th17 cells, performed on RNA-seq datasets. The total height of the curve reflects the extent of enrichment (ES). The normalized enrichment score (NES), the false discovery rate (FDR), and the p-value are indicated.

Author Manuscript Author Manuscript Author Manuscript Author Manuscript

(**D–E**) GM-CSF (**D**) and IL-10 (**E**) production by $CD4^+$ T cells activated in the presence of indicated cytokine combinations for 4 days, assayed by flow-cytometry (n=4–5 samples for **D** and n=6–7 for **E** from 3 experiments; ns, not significant, **p<0.01, two-sided *t*-test; center bars indicate mean values)

(**F**) Schema of adoptive transfer of 2D2 T cells activated in the presence of IL-6, Activin-A +IL-6 or TGF-β1+IL-6 into irradiated recipient mice to induce EAE.

(**G–H**) The comparison of the EAE incidence (**G**), clinical scores (left panel), and the linear-regression analysis (right panel) (**H**) of the recipient mice depicted in **F**. (n=9 mice in each group from 3 experiments; mean ± s.e.m., **p<0.01, ***p<0.001, two-way multiple-range ANOVA test)

(**I**) IL-10 production by $CD4^+$ T cells infiltrating in the spinal cords of mice with EAE as in **G–H**, assayed by flow-cytometry (n=5 samples from 3 experiments; *p<0.05, two-sided *t*-test; center bars indicate mean values)

Author Manuscript Author Manuscript Author Manuscript Author Manuscript

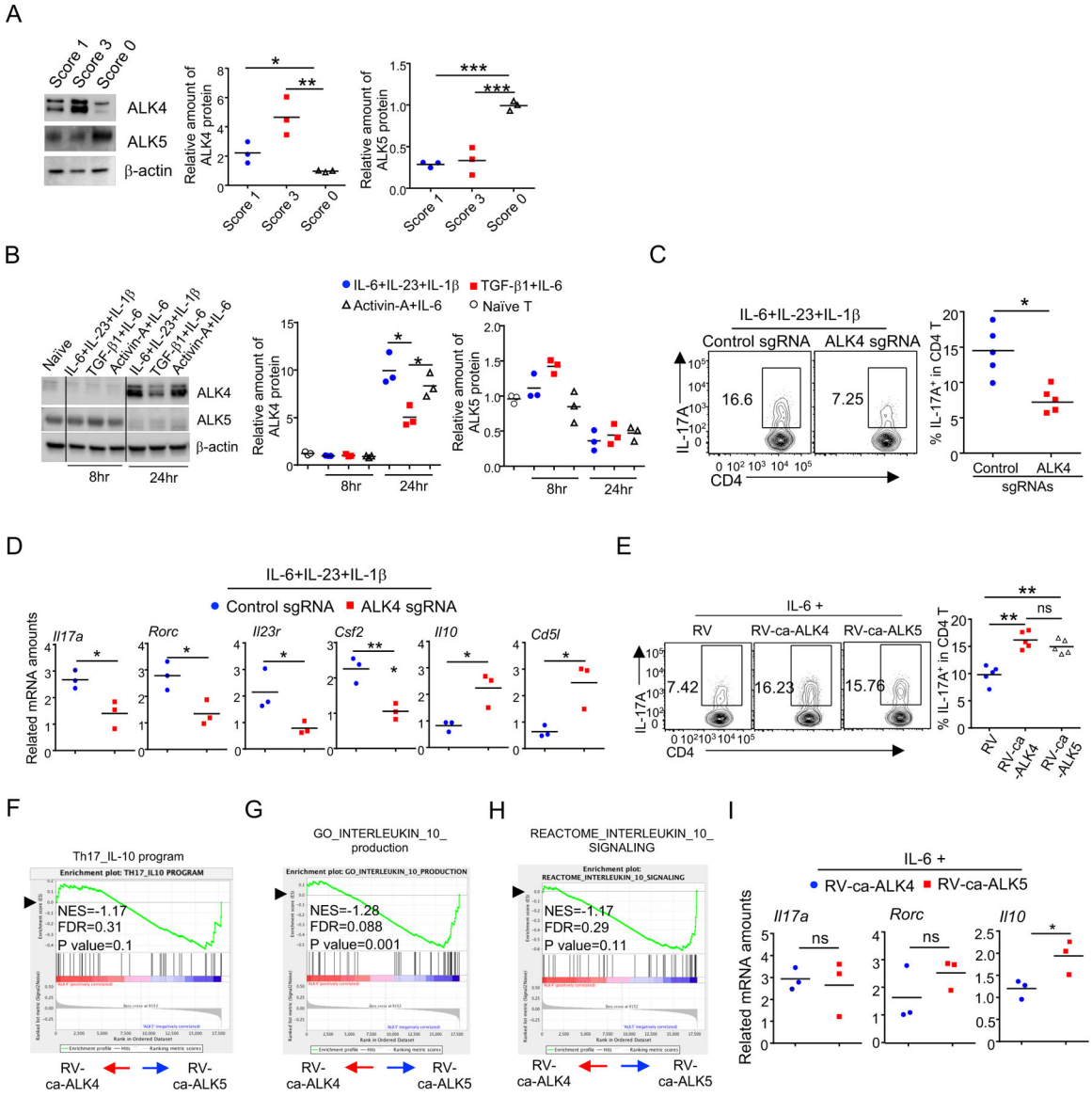

Figure 5. ALK4 and ALK5 functioned differently in directing Th17 cell differentiation *in vitro*.
See also Figure S4.

A) Immuno-blotting to detect Activin-A receptor type I (ALK4) and TGFβ receptor type I (ALK5) protein expression in $CD4^+$ T cells infiltrating in the spinal cords of EAE-inflicted mice. The relative ALK4 and ALK5 protein amounts were determined by densitometry. (n=3 experiments; *p<0.05, **p<0.01, ***p<0.001, two-sided *t*-test; center bars indicate mean values)

(**B**) Immuno-blotting to detect ALK4 and ALK5 protein expression in $CD4^+$ T cells activated in the presence of indicated cytokine combinations, at indicated time points. The relative ALK4 and ALK5 protein amounts were determined by densitometry. (n=3 experiments; *p<0.05, two-sided *t*-test; center bars indicate mean values)

(**C**) $CD4^+$ T cells from *Cd4Cre;Cas9* mice were activated in the presence of IL-6+IL-23+IL-1β and transduced with lentivirus expressing control sgRNA or ALK4

Author Manuscript Author Manuscript Author Manuscript Author Manuscript

sgRNA together with Thy1.1. IL-17A production by transduced (Thy1.1$^+$) cells was assayed by flow-cytometry 4 days after transduction. (n=5 samples from 3 experiments; *p<0.05, two-sided *t*-test; center bars indicate mean values)

(**D**) mRNA expression of Th17-related genes in transduced (Thy1.1$^+$) CD4$^+$ T cells as in **C**, assayed by qRT-PCR. (n=3 samples from 3 experiments; *p<0.05, **p<0.01, two-sided *t*-test; center bars indicate mean values)

(**E**) CD4$^+$ T cells were activated in the presence of IL-6 and transduced by MSCV retrovirus (RV) encoding constitutive active ALK4 (RV-ca-ALK4) or constitutive active ALK5 (RV-ca-ALK5) together with Thy1.1. IL-17A production by transduced (Thy1.1$^+$) cells was determined by flow-cytometry 4 days after transduction. (n=5 samples from 3 experiments; ns, not significant, **p<0.01, two-sided *t*-test; center bars indicate mean values)

(**F–H**) Gene set enrichment analysis (GSEA) of Th17-IL-10 program defined in a previous study (Aschenbrenner et al., 2018) (**F**), GO_INTERLEUKIN_10_PRODUCTION gene set (**G**), and REACTOME_INTERLEUKIN_10_SIGNALING gene set (**H**) in RV-ca-ALK4- vs RV-ca-ALK5-transduced CD4$^+$ T cells described in **E**, performed on RNA-seq datasets. The total height of the curve reflects the extent of enrichment (ES). The normalized enrichment score (NES), the false discovery rate (FDR), and the p-value are indicated.

(**I**) mRNA expression of *Il17a, Rorc*, and *Il10* in RV-ca-ALK4 and RV-ca-ALK5 transduced CD4$^+$ T cells described in **E**, assayed by qRT-PCR. (n=3 samples from 3 experiments; ns, not significant, *p<0.05, two-sided *t*-test; center bars indicate mean values)

Author Manuscript Author Manuscript Author Manuscript Author Manuscript

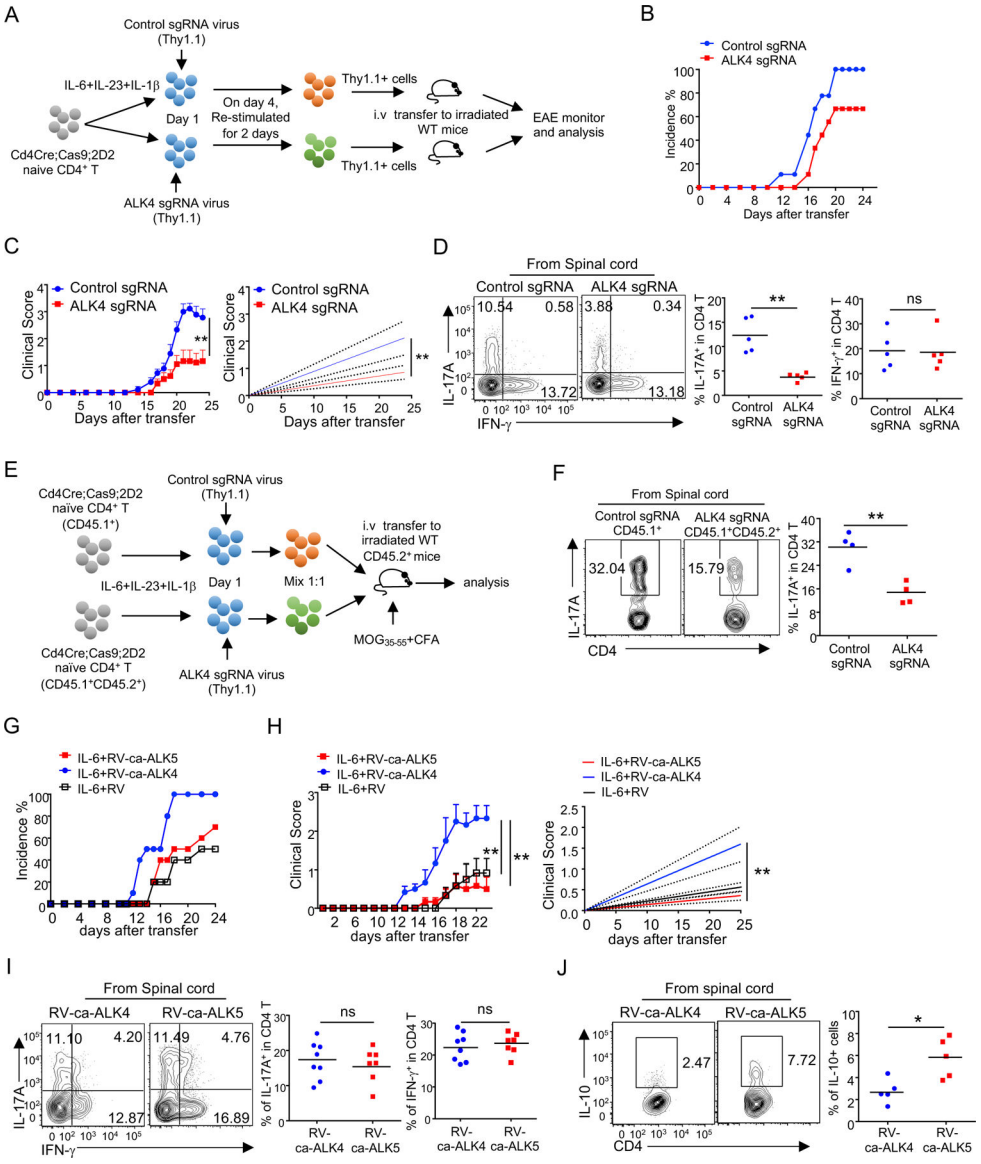

Figure 6. ALK4 was critical for pathogenic-Th17 cell elicited neuroinflammation.

(**A**) Schema of adoptive transfer of 2D2 T cells to elicit EAE disease. CD4$^+$ T cells from *Cd4Cre;Cas9;2D2* mice were activated in the presence of IL-6+IL-23+IL-1β and transduced with lentivirus expressing ALK4 sgRNA or control sgRNA together with Thy1.1. T cells were re-stimulated for 2 days without cytokines. 1×10^6 transduced (Thy1.1$^+$) T cells were purified and i.v injected to 400 cGy irradiated recipient mice to induce EAE.

(**B–C**) The comparison of the EAE incidence (**B**), clinical scores (**C**, left panel), and the linear-regression analysis (**C**, right panel) of mice that received different T cells depicted in **A**. (n=9 for each group from 3 experiments; mean ± s.e.m., **p<0.01, two-way multiple-range ANOVA test)

(**D**) IL-17A and IFN-γ production by control sgRNA and ALK4 sgRNA transduced CD4$^+$ T cells infiltrating in the spinal cords of EAE-inflicted mice, assayed by flow-cytometry (n=5

Author Manuscript Author Manuscript Author Manuscript Author Manuscript

samples from 3 experiments; ns, not significant; **p<0.01, two-sided *t*-test; center bars indicate mean values)

(**E**) Schema of adoptive transfer of both control sgRNA transduced T cells ($CD45.1^+$) and ALK4 sgRNA transduced T cells ($CD45.1^+CD45.2^+$) into irradiated recipient mice ($CD45.2^+$), where EAE was elicited with $MOG_{35–55}$+CFA.

(**F**) IL-17A production by control sgRNA transduced and ALK4 sgRNA transduced $CD4^+$ T cells infiltrating in the spinal cords of EAE-inflicted mice as in **E**, assayed by flow-cytometry of (n=4 samples from 3 experiments; **p<0.01, two-sided *t*-test; center bars indicate mean values)

(**G–H**) $CD4^+$ T cells from 2D2 mice were activated in the presence of IL-6 and transduced with MSCV retrovirus (RV), MSCV retrovirus expressing ca-ALK4 (RV-ca-ALK4) or ca-ALK5 (RV-ca-ALK5) together with Thy1.1 for 4 days. Transduced ($Thy1.1^+$) T cells were purified and transferred into irradiated wild-type mice to induce EAE. The EAE incidence (**G**), clinical scores (**H**, left panel) and the linear-regression analysis (**H**, right panel) of the mice received different T cells were compared. (n=10 for each group from 3 experiments; mean ± s.e.m., **p<0.01, two-way multiple-range ANOVA test)

(**I**) IL-17A and IFN-γ production by ca-ALK4 and ca-ALK5-transduced $CD4^+$ T cells infiltrating in the spinal cords of EAE-inflicted mice described in **G-H**, assayed by flow-cytometry of (n=7–8 samples from 3 experiments; ns, not significant, two-sided *t*-test; center bars indicate mean values)

(**J**) IL-10 production by RV-ca-ALK4 and RV-ca-ALK5-transduced $CD4^+$ T cells infiltrating in the spinal cords of EAE-inflicted mice described in **G-H**, assayed by flow-cytometry. (n=5 samples from 3 experiments; *p<0.05, two-sided *t*-test; center bars indicate mean values)

Author Manuscript Author Manuscript Author Manuscript Author Manuscript

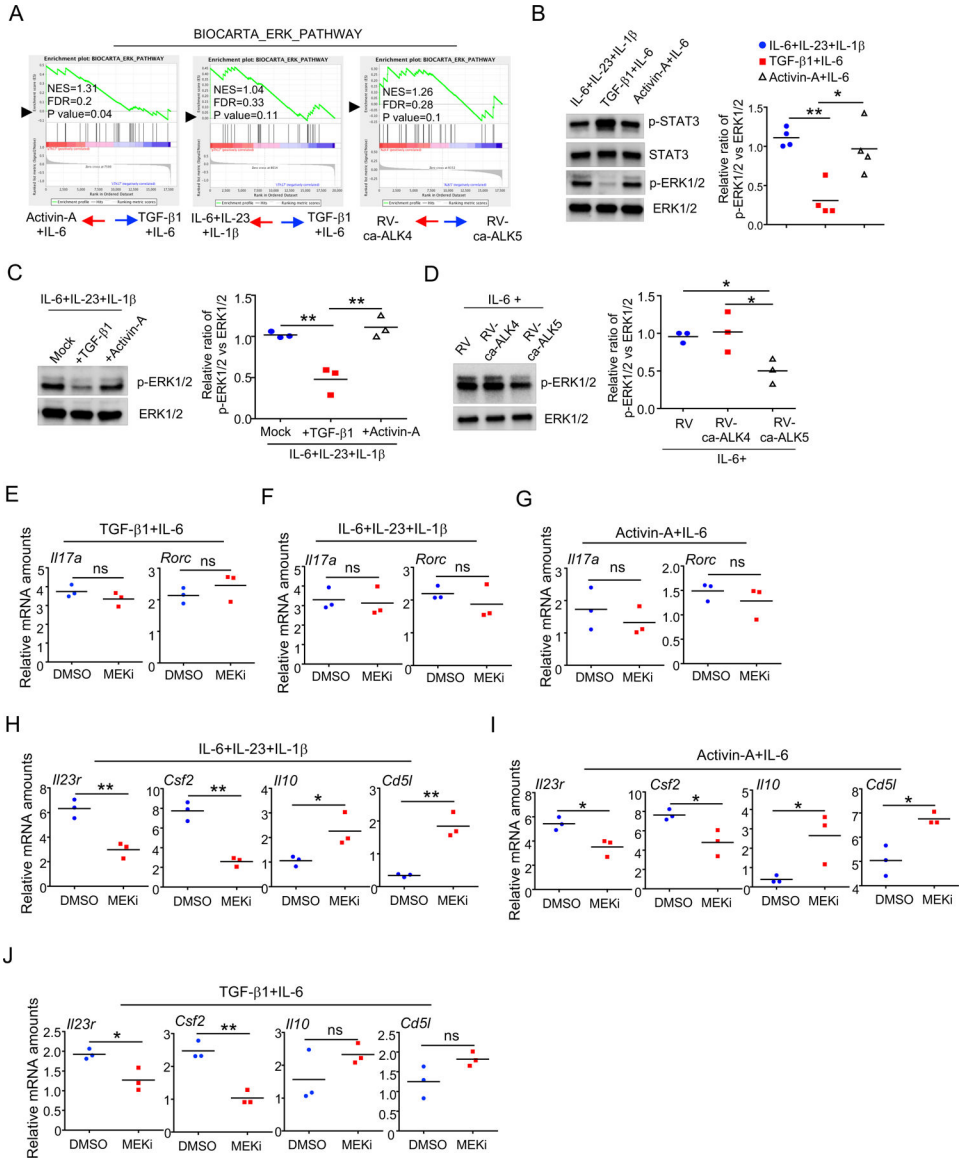

Figure 7. TGF-β1-ALK5, but not Activin-A-ALK4, suppressed ERK activation that was important for Th17 cells to gain pathogenic program.

See also Figure S5.

(**A**) Gene set enrichment analysis (GSEA) of BIOCARTA_ERK_PATHWAY in activated CD4$^+$ T cells that were treated with indicated cytokine combinations or transduced with RV-ca-ALK4 or RV-ca-ALK5 in the presence of IL-6, performed on RNA-seq datasets. The total height of the curve reflects the extent of enrichment (ES). The normalized enrichment score (NES), the false discovery rate (FDR), and the p-value are indicated.

(**B**) Immuno-blotting to detect p-ERK1/2, ERK1/2, p-STAT3 and STAT3 protein expression in CD4$^+$ T cells activated in the presence of indicated cytokines combinations for 2 days. The relative ratios of p-ERK1/2 vs. ERK1/2 protein amounts were determined by densitometry. (n=4 experiments; *p<0.05, **p<0.01, two-sided *t*-test; center bars indicate mean values)

Author Manuscript Author Manuscript Author Manuscript Author Manuscript

(**C**) Immuno-blotting to detect p-ERK1/2 and ERK1/2 protein expression in $CD4^+$ T cells activated in the presence of IL-6+IL-23+IL-1β and 1 ng/ml TGF-β1 or 30 ng/ml Activin-A for 2 days. The relative ratios of p-ERK1/2 vs. ERK1/2 protein amounts were determined by densitometry. (n=3 experiments; **p<0.01, two-sided *t*-test; center bars indicate mean values)

(**D**) Immuno-blotting to detect p-ERK1/2 and ERK1/2 protein expression in $CD4^+$ T cells transduced with RV-ca-ALK4 or RV-ca-ALK5 in the presence of IL-6 for 4 days. The relative ratios of p-ERK1/2 vs. ERK1/2 protein amounts were determined by densitometry. (n=3 experiments; *p<0.05, two-sided *t*-test; center bars indicate mean values)

(**E–G**) mRNA expression of *Il17a* and *Rorc* in $CD4^+$ T cells activated in the presence of TGF-β1+IL-6 (**E**), IL-6+IL-23+IL-1β (**F**), and Activin-A+IL-6 (**G**), with 10 μM MEK inhibitor (MEKi) or without (DMSO) for 4 days, assayed by qRT-PCR (n=3 samples from 3 experiments; ns, not significant, two-sided *t*-test; center bars indicate mean values)

(**H–J**) mRNA expression of *Csf2, Il-23r*, *Il10* and *Cd5l* in $CD4^+$ T cells activated in the presence of IL-6+IL-23+IL-1β (**H**), Activin-A+IL-6 (**I**), and TGF-β1+IL-6 (**J**), with 10 μM MEK inhibitor (MEKi) or without (DMSO) for 4 days, assayed by qRT-PCR. (n=3 samples from 3 experiments; ns, not significant, *p<0.05, **p<0.01, two-sided *t*-test; center bars indicate mean values)

Author Manuscript Author Manuscript Author Manuscript Author Manuscript

KEY RESOURCES TABLE

REAGENT or RESOURCE	SOURCE	IDENTIFIER
Antibodies		
Pacific Blue anti-mouse CD4	Biolegend	Cat# 100531 RRID:AB_493646
PE anti-mouse IL-10	Biolegend	Cat# 505008 RRID:AB_315362
FITC anti-mouse IL-10	Biolegend	Cat# 505006 RRID:AB_315360
APC anti-mouse IL-17A	Biolegend	Cat# 506916 RRID:AB_536018
PE anti-mouse IL-17A	Biolegend	Cat# 506904 RRID:AB_315464
FITC anti-mouse CD45.1	Biolegend	Cat# 110706 RRID: AB_313494
FITC anti-mouse CD45.2	Biolegend	Cat# 109806 RRID:AB_313443
FITC anti-mouse GM-CSF	Biolegend	Cat# 505404 RRID:AB_ 315380
FITC anti-mouse IFN-γ	Biolegend	Cat# 505806 RRID:AB_315400
PE anti-mouse Thy1.1	Biolegend	Cat# 205903 RRID:AB_2561424
Anti-mouse ALK4	Abcam	Cat#ab109300 RRID:AB_10860328
Anti-mouse ALK5	Abcam	Cat# ab31013, RRID:AB_778352
Smad2 (D43B4) XP® Rabbit mAb	Cell Signal Technology	Cat# 5339, RRID:AB_10626777
Phospho-Smad2 (Ser465/Ser467)	Cell Signal Technology	Cat# 18338, RRID:AB_2798798
Anti-mouse Phospho-STAT3	Cell Signal Technology	Cat# 9138 RRID: AB_331262
Anti-mouse STAT3	Cell Signal Technology	Cat# 9139, RRID:AB_331757
Anti-mouse Phospho-ERK1/2	Cell Signal Technology	Cat# 9101 RRID:AB_331646
Anti-mouse ERK1/2	BD Bioscience	Cat# 610123 RRID: AB_397529
Anti-mouse SKI	Santa Cruz	Cat# sc-271916, RRID:AB_10610623
Anti-mouse β-actin	Santa Cruz	Cat# SC-1616 RRID:AB_630836
*In Vivo*MAb anti-mouse CD3	BioXcell	Cat# BE0002, RRID:AB_1107630
*In Vivo*MAb anti-mouse CD28	BioXcell	Cat# BE0015–1, RRID:AB_1107624
*In Vivo*MAb anti-mouse IFN-γ	BioXcell	Cat# BE0055, RRID:AB_1107694
*In Vivo*MAb Anti-mouse TGF-β1	BioXcell	Cat# BE0057, RRID:AB_1107757
Mouse Activin-A beta A subunit Antibody	R&D	Cat# MAB3381–100 RRID:AB_2125864
donkey anti-mouse IgG-HRP	Santa Cruz	Cat# SC-2314, RRID:AB_641170
donkey anti-rabbit IgG-HRP	Santa Cruz	Cat# SC-2313, RRID:AB_641181
donkey anti-goat IgG-HRP	Santa Cruz	Cat# SC-2020, RRID:AB_631728
Biological Samples		
Fetal Bovine Serum	Corning	Cat# 35–015-CV
Chemicals, Peptides, and Recombinant Proteins		
Recombination Follistatin	R&D	Cat# 769-FS-025
Recombination Activin-A	Biolegend	Cat# 592004

Author Manuscript Author Manuscript Author Manuscript Author Manuscript

REAGENT or RESOURCE	SOURCE	IDENTIFIER
Recombination IL-1β	Biolegend	Cat# 575106
Recombination IL-6	Biolegend	Cat# 575706
Recombination IL-23	Biolegend	Cat# 589006
Recombination TGF-β1	Biolegend	Cat# 580704
PBS (Phosphate buffered saline)	Homemade	N/A
Ammonium-Chloride-Potassium (ACK) Lysing Buffer	Homemade	N/A
CD4 (L3T4) MicroBeads, mouse	Miltenyi Biotec	Cat# 130–117-043 RRID:AB_2722753
Collagenase D	Sigma	Cat# 11088866001
Percoll	Sigma	Cat# P-4937
HEPES buffer	Gibco	Cat# 15630080
Heparin	Sigma	Cat# H3393
Fixation/Permeabilization Solution Kit	BD Bioscience	Cat# 554714
7-AAD (7-Aminoactinomycin D)	BD Bioscience	Cat# 559925 RRID:AB_2869266
PE Annexin V	BD Bioscience	Cat# 556422 RRID:AB_2869071
TGFβRI inhibitor SB525334	Selleckchem	Cat# S1476
MEK inhibitor PD98059	Selleckchem	Cat# S1177
carboxyfluorescein diacetate succinimidyl ester (CFSE)	AnaSpec	Cat# AS-89000
Incomplete Freund's adjuvant	Difco Laboratories	Cat# BD™ 263910
Mycobacterium tuberculosis H37RA	Difco Laboratories	Cat# BD™ 231141
Murine myelin oligodendrocyte glycoprotein (MOG) peptide 35–55	AnaSpec	Cat# AS-60130–1
X-VIVO 20 medium	Lonza	Cat# 04–448QT
DMEM medium	Gbico	Cat# 12430112
penicillin-streptomycin	Gbico	Cat# 10378016
phorbol 12-myristate 13-acetate (PMA)	Sigma	Cat# P8139
ionomycin	Sigma	Cat# I3909
Puromycin	ThermoFisher	Cat# A1113802
Brefeldin A	eBioscience	Cat# 00–4506-51
FuGENE transfection reagent	Promega	Cat# E2692
Polybrene	Sigma	Cat# TR-1003
Pertussis toxin	List Biological	Cat# 180
TRizol	Invitrogen	Cat# 15596026
iTaq Universal Probes Supermix	Bio-Rad	Cat# 1725134
RIPA lysis buffer	Sigma	Cat# R0278
polyvinylidene fluoride membrane	Bio-Rad	Cat# 1620177
Any kD™ Mini-PROTEAN® TGX™ Precast Protein Gels	Bio-Rad	Cat# 4569033
SuperSignal™ West Pico PLUS Chemiluminescent Substrate	ThermoFisher	Cat# 34579
Critical Commercial Assays		
Direct-zol RNA Miniprep	ZYMO Research	Cat# R2051

Author Manuscript Author Manuscript Author Manuscript Author Manuscript

REAGENT or RESOURCE	SOURCE	IDENTIFIER
iScriptTM cDNA Synthesis Kit	Bio-Rad	Cat# 1708891
Human/Mouse/Rat Activin-A Quantikine ELISA Kit	R&D	Cat# DAC00B
Deposited Data		
RNA sequencing data	This Paper	GSE151533
Experimental Models: Cell Lines		
HEK293T cells	ATCC	Cat# CRL-3216, RRID:CVCL_0063
Experimental Models: Organisms/Strains		
Mouse: C57BL/6J (CD45.2)	The Jackson Laboratory	Cat# JAX:000664, RRID:IMSR_JAX:000664
Mouse: B6.SJL-PtprcaPepcb/BoyCrl (CD45.1)	Charles River	Cat# CRL:494, RRID:IMSR_CRL:494
Mouse: B6.Cg-Tg(Cd4-cre)1Cwi/BfluJ	The Jackson Laboratory	Cat# JAX:022071, RRID:IMSR_JAX:022071
Mouse: *CD4cre*-dependent-*Cas9*-expressing	Platt et al., 2014	N/A
Mouse: C57BL/6-Tg (Tcra2D2, Tcrb2D2)1Kuch/J	The Jackson Laboratory	Cat# JAX006912 RRID:IMSR_JAX:006912
Oligonucleotides		
Activin-A sgRNA: ACCCCAGGATCCGAGGGGCA	This paper	N/A
ALK4 sgRNA: GTTACTATGGCGGAGTCGGC	This paper	N/A
Recombinant DNA		
FST cDNA	Transomics	Cat# BC145945
ALK4 T206D cDNA	Dharmacon	Clone ID:40131078
ALK5 T204D cDNA	Dharmacon	Clone ID:6409765
MSCV-IRES-Thy1.1 (MIT)	Wu et al. 2006	Cat# 17442, Addgene
pLKO.1-scramble shRNA control	Moffat et al. 2006	Cat# 10878, Addgene
MIT-FST	This paper	N/A
MIT-ca-ALK4	This paper	N/A
MIT-ca-ALK5	This paper	N/A
pCL-Eco	Naviaux et al, 1996	Cat# 12371, Addgene
pMD2.G	a gift from Didier Trono	Cat# 12259, Addgene
psPAX2	a gift from Didier Trono	Cat# 12260, Addgene
Activin-A shRNA clone #1	Sigma	Cat# TRCN0000067739
Activin-A shRNA clone #2	Sigma	Cat# TRCN0000067740
lentis-U6-sgRNA-SFFV-Cas9-Thy1.1	This paper	N/A
Lentivirus expressing Activin-A sgRNA	This paper	N/A
Lentivirus expressing ALK4 sgRNA	This paper	N/A
Software and Algorithms		
FlowJo, v7.0	FlowJo, Treestar Inc.	https://www.flowjo.com RRID: SCR_008520
PRISM, v7	GraphPad Software	https://www.graphpad.com/scientific-software/prism/ RRID: SCR_002798
Image J	Schneider et al., 2012	https://imagej.nih.gov/ij/
CHOPCHOP	N/A	https://chopchop.cbu.uib.no
STAR, Version 2.5.1	N/A	https://github.com/alexdobin/STAR

Author Manuscript

Author Manuscript

Author Manuscript

Author Manuscript

REAGENT or RESOURCE	SOURCE	IDENTIFIER
featureCount, Version 1.4.6	Subread	http://subread.sourceforge.net
Bioconductor package, DESeq2	N/A	http://bioconductor.org/packages/release/bioc/html/DESeq2.html
R, Version 3.6.3	N/A	https://rstudio.com
Partek, Version 7.2,	N/A	https://www.partek.com
GSEA, V4.0.3,	Broad Institute	https://www.gsea-msigdb.org/gsea/index.jsp
Others		
BD Vacutainer blood collection tubes	BD Biosciences	Cat#367871